Interval Type-2 Fuzzy Logic Systems: Theory and Design

Qilian Liang and Jerry M. Mendel, *Fellow, IEEE*

***Abstract*—In this paper, we present the theory and design of interval type-2 fuzzy logic systems (FLSs). We propose an efficient and simplified method to compute the input and antecedent operations for interval type-2 FLSs; one that is based on a general inference formula for them. We introduce the concept of upper and lower membership functions (MFs) and illustrate our efficient inference method for the case of Gaussian primary MFs. We also propose a method for designing an interval type-2 FLS in which we tune its parameters. Finally, we design type-2 FLSs to perform time-series forecasting when a nonstationary time-series is corrupted by additive noise where SNR is uncertain and demonstrate improved performance over type-1 FLSs.**

***Index Terms*—Interval type-2 fuzzy sets, nonsingleton fuzzy logic systems, time-series forecasting, tuning of parameters, type-2 fuzzy logic systems, upper and lower membership functions.**

I. Introduction

A FUZZY logic system (FLS) (also known as a fuzzy system, fuzzy logic controller, etc) includes fuzzifier, rules, inference engine, and defuzzifier [22]. Quite often, the knowledge that is used to construct the rules in a FLS is uncertain. Three ways in which such rule uncertainty can occur are: 1) the words that are used in antecedents and consequents of rules can mean different things to different people [23]; 2) consequents obtained by polling a group of experts will often be different for the same rule because the experts will not necessarily be in agreement; and 3) noisy training data. Antecedent or consequent uncertainties translate into uncertain antecedent or consequent membership functions. Type-1 FLSs, whose membership functions are type-1 fuzzy sets, are unable to directly handle rule uncertainties. Type-2 FLSs, the subject of this paper, in which antecedent or consequent membership functions are type-2 fuzzy sets, can handle rule uncertainties.

The concept of type-2 fuzzy sets was introduced by Zadeh [41] as an extension of the concept of an ordinary fuzzy set, i.e., a type-1 fuzzy set. Type-2 fuzzy sets have grades of membership that are themselves fuzzy [4]. A type-2 membership grade can be any subset in $[0, 1]$—the *primary membership*; and, corresponding to each primary membership, there is a *secondary membership* (which can also be in $[0, 1]$) that defines the possibilities for the primary membership. A type-1 fuzzy set is a special case of a type-2 fuzzy set; its secondary membership function is a subset with only one element—unity. Type-2 fuzzy sets allow us to handle linguistic uncertainties, as typified by the adage "words can mean different things to different people." A fuzzy relation of higher type (e.g., type-2) has been regarded as one way to increase the fuzziness of a relation and, according to Hisdal, "increased fuzziness in a description means increased ability to handle inexact information in a logically correct manner [6]."

Mizumoto and Tanaka [25] studied the set theoretic operations of type-2 sets, properties of membership grades of such sets, and examined the operations of algebraic product and algebraic sum for them [26]. More details about algebraic structure of type-2 sets are given in [28]. Dubois and Prade [2]–[4] discussed fuzzy valued logic and give a formula for the composition of type-2 relations as an extension of the type-1 sup-star composition, but this formula is only for minimum t-norm. A general formula for the extended sup-star composition of type-2 relations is given by Karnik and Mendel [11], [12], [17]. Based on this formula, Karnik and Mendel [10]–[12], [17] established a complete type-2 FLS theory to handle uncertainties in FLS parameters.

Similar to a type-1 FLS, a type-2 FLS includes fuzzifier, rule base, fuzzy inference engine, and output processor. The output processor includes type-reducer and defuzzifier; it generates a type-1 fuzzy set output (from the type-reducer) or a crisp number (from the defuzzifier). A type-2 FLS is again characterized by IF–THEN rules, but its antecedent or consequent sets are now type-2. Type-2 FLSs can be used when the circumstances are too uncertain to determine exact membership grades such as when training data is corrupted by noise—a case studied later in this paper.

General type-2 FLSs are computationally intensive because type-reduction is very intensive. Things simplify a lot when secondary membership functions (MFs) are interval sets (in this case, the secondary memberships are either zero or one and we call them interval type-2 sets) and this is the case studied in this paper. When the secondary MFs are interval sets, we call the type-2 FLSs "interval type-2 FLSs." For some other discussions on the use of interval sets in fuzzy logic (see Hisdal [6], Schwartz [32], and Turksen [34]).

The most commonly used fuzzifier is a singleton; but, such a fuzzifier is not adequate when data is corrupted by measurement noise. In this case, a nonsingleton fuzzifier that treats each measurement as a fuzzy number should be used. The theory and applications of a type-1 FLS with nonsingleton fuzzifier are presented in [27], where the input is fuzzified into a type-1 fuzzy set (e.g., Gaussian) whose parameters are based on the measured input and the mean and variance of the measurement noise. This assumes that the statistical knowledge (mean and variance) of

Manuscript received August 20, 1999; revised May 30, 2000.

The authors are with the Signal and Image Processing Institute, Department of Electrical Engineering Systems, University of Southern California, Los Angeles, CA 90089-2564 USA (e-mail: mendel@sipi.usc.edu).

Publisher Item Identifier S 1063-6706(00)08455-1.

the noise is given or can be estimated; but, in many cases, these values are not known ahead of time and can not be estimated from the data. Instead, we only have some linguistic knowledge about the noise, such as *very noisy*, *moderately noisy*, or *approximately no noise*. In this case, we cannot fuzzify the crisp input as a type-1 fuzzy set, because type-1 MFs cannot fully represent the uncertainty associated with this linguistic knowledge. We believe that in this important case, *the input should be fuzzified into a type-2 fuzzy set* for use in a nonsingleton type-2 FLS. This case is also studied in this paper.

In this paper, we also provide a design method for an interval type-2 FLS, where IF–THEN fuzzy rules are obtained from given input–output (I/O) data. Two primary design tasks are *structure identification* and *parameter adjustment* [7]. The former determines input/output (I/O) space partition, antecedent and consequent variables, the number of IF–THEN rules (which are determined by the I/O space partition), and the number and initial locations of membership functions. The latter identifies a feasible set of parameters under the given structure. In this paper, we focus on *parameter adjustments* in an interval type-2 FLS.

Tuning the parameters of a type-1 FLS is possible because its output $f(\mathbf{x})$ can be expressed as a closed-form mathematical formula. Optimization methods for doing this have been extensively studied (for example, [7], [19], [22], [24], and [36]). Unfortunately, the output of a type-2 FLS cannot be represented by a closed-form mathematical formula; hence, there is an additional level of complexity associated with tuning its parameters.

To date, type-2 sets and FLSs have been used in decision making [1], [40], solving fuzzy relation equations [35], survey processing, [12], [13], time-series forecasting [12], [14], function approximation [12], time-varying channel equalization [17], control of mobile robots [39], and preprocessing of data [9].

In the sequel, results for a general type-2 nonsingleton fuzzy logic system (NSFLS) are given in Section II; *meet* and *join* operations for interval sets are given in Section III; upper and lower membership functions that characterize a type-2 MF are introduced in Section IV; an efficient and simplified method to compute the input and antecedent operations for interval type-2 FLSs is given in Section V; type-reduction and defuzzification for an interval type-2 FLS are reviewed in Section VI; a method for designing an interval type-2 FLS is given in Section VII; an application of our design method is given in Section VIII for time-series forecasting of a nonstationary time-series that is corrupted by additive noise whose SNR is uncertain; and, finally, the conclusions and topics for future research are given in Section IX.

In this paper, A denotes a type-1 fuzzy set; $\mu_A(x)$ denotes the membership grade of x in the type-1 fuzzy set A; $\tilde{A}$ denotes a type-2 fuzzy set; $\mu_{\tilde{A}}(x)$ denotes the membership grade of x in the type-2 fuzzy set $\tilde{A}$, i.e., $\mu_{\tilde{A}}(x) = \int_u f_x(u)/u$, $u \in J \subseteq [0, 1]$; $\sqcap$ denotes *meet* operation; and, $\sqcup$ denotes *join* operation. Meet and join are defined and explained in great detail in [10]–[12], [15].

II. Type-2 FLSs: General Results

In a type-2 FLS with a rule base of M rules in which each rule has p antecedents, let the lth rule be denoted by R^l, where R^l: IF x_1 is $\tilde{F}_1^l$, x_2 is $\tilde{F}_2^l$, …, and x_p is $\tilde{F}_p^l$, THEN y is $\tilde{G}^l$. The membership function $\mu_{\tilde{B}^l}(y)$ of a fired rule can be expressed by the following extended sup-star composition [12], [17]:

$$\mu_{\tilde{B}^l}(y) = \sqcup_{\mathbf{x}\in X}\left[\mu_{\tilde{A}_x}(\mathbf{x}) \sqcap \mu_{\tilde{A}^l \to \tilde{B}^l}(\mathbf{x}, y)\right] \tag{1}$$

where X is a p-dimensional Cartesian product space, $X = X_1 \times \cdots \times X_p$, X_k is the measurement domain of input x_k, ($k = 1, \ldots, p$); and $\tilde{A}_x$ is given by

$$\mu_{\tilde{A}_x}(\mathbf{x}) = \mu_{\tilde{X}_1 \times \cdots \times \tilde{X}_p}(\mathbf{x}) = \mu_{\tilde{X}_1}(x_1) \sqcap \ldots \sqcap \mu_{\tilde{X}_p}(x_p). \tag{2}$$

Additionally

$$\mu_{\tilde{A}^l \to \tilde{G}^l}(\mathbf{x}, y) = \mu_{\tilde{F}_1^l}(x_1) \sqcap \mu_{\tilde{F}_2^l}(x_2) \sqcap \ldots \sqcap \mu_{\tilde{F}_p^l}(x_p) \sqcap \mu_{\tilde{G}^l}(y). \tag{3}$$

Substituting (3) and (2) into (1), the latter becomes

$$\mu_{\tilde{B}^l}(y) = \mu_{\tilde{G}^l}(y) \sqcap \left\{\sqcup_{\mathbf{x}\in X}\left\{\left[\mu_{\tilde{X}_1}(x_1) \sqcap \mu_{\tilde{F}_1^l}(x_1)\right] \sqcap \ldots \sqcap \left[\mu_{\tilde{X}_p}(x_p) \sqcap \mu_{\tilde{F}_p^l}(x_p)\right]\right\}\right\}, \qquad y \in Y. \tag{4}$$

Let

$$\mu_{\tilde{Q}_k^l}(x_k) \triangleq \mu_{\tilde{X}_k}(x_k) \sqcap \mu_{\tilde{F}_k^l}(x_k) \tag{5}$$

then

$$\mu_{\tilde{B}^l}(y) = \mu_{\tilde{G}^l}(y) \sqcap \left\{\sqcup_{\mathbf{x}\in X}\left[\sqcap_{k=1}^p \mu_{\tilde{Q}_k^l}(x_k)\right]\right\}, \qquad y \in Y. \tag{6}$$

Suppose that any N of the M rules in the FLS fire, where $N \leq M$; then, the output fuzzy set, $\mu_{\tilde{B}}(y)$ for a type-2 FLS is

$$\mu_{\tilde{B}}(y) = \sqcup_{l=1}^N \mu_{\tilde{B}^l}(y), \qquad y \in Y. \tag{7}$$

For later use, we define

$$\mu_{\tilde{Q}^l}(\mathbf{x}) \triangleq \sqcap_{k=1}^p \mu_{\tilde{Q}_k^l}(x_k) \tag{8}$$

and

$$F^l \triangleq \sqcup_{\mathbf{x}\in X}\left[\sqcap_{k=1}^p \mu_{\tilde{Q}_k^l}(x_k)\right] = \sqcup_{\mathbf{x}\in X} \mu_{\tilde{Q}^l}(\mathbf{x}) \tag{9}$$

so that (6) can be re-expressed as

$$\mu_{\tilde{B}^l}(y) = \mu_{\tilde{G}^l}(y) \sqcap F^l \qquad y \in Y. \tag{10}$$

General type-2 FLSs are computationally intensive. Things simplify a lot when secondary MFs are interval sets, in which case secondary memberships are either zero or one and, as we demonstrate below, such simplifications make the use of type-2 FLSs practical.

III. Meet and Join for Interval Sets

The *meet* and *join* operations, which are needed in (5)–(10), can be greatly simplified for interval type-1 sets.

Theorem 1 (Meet of Interval Sets Under Minimum or Product t-Norms):

a) Let $F = \int_{v\in F} 1/v$ and $G = \int_{w\in G} 1/w$ be two interval type-1 sets (often called interval sets) with domains $v \in$

$[l_f, r_f]$ ($[l_f, r_f] \subseteq [0, 1]$), and $g \in [l_g, r_g]$ ($[l_g, r_g] \subseteq [0, 1]$), respectively. The *meet* between F and G, $Q = F \sqcap G$ ($Q = \int_{v \in Q} 1/q$), under minimum or product t-norms (i.e., $\star$) is given by

$$Q = F \sqcap G = \int_{q \in [l_f \star l_g, r_f \star r_g]} 1/q \tag{11}$$

where $q = v \star w$.

b) The *meet* under minimum or product t-norms of n interval type-1 sets $F_1, \ldots, F_n$, $\sqcap_{i=1}^{n} F_i$, having domains $[l_1, r_1], \ldots, [l_n, r_n]$, respectively, where $[l_i, r_i] \subseteq [0, 1]$ $i = 1, 2, \ldots, n$ is an interval set with domain $[(l_1 \star l_2 \star \cdots \star l_n), (r_1 \star r_2 \star \cdots \star r_n)]$.

The proof of Theorem 1a), based on minimum or product operations between two interval sets, is given in [18] and [32]. The extension to part b) (via mathematical induction) is so straightforward, we leave it to the reader.

Theorem 2 (Join of Interval Sets):

a) Let F and G be as defined in part (a) of Theorem 1. The *join* between F and G, $Q = F \sqcup G$ ($Q = \int_{v \in Q} 1/q$), is given by

$$Q = F \sqcup G = \int_{q \in [l_f \vee l_g, r_f \vee r_g]} 1/q \tag{12}$$

where $q = v \vee w$.

b) Let F_i ($i = 1, 2, \ldots, n$) be as defined in Theorem 1(b). Then the *join* of these n interval type-1 sets is an interval set with domain $[(l_1 \vee l_2 \vee \cdots \vee l_n), (r_1 \vee r_2 \vee \cdots \vee r_n)]$. The proof of Theorem 2(a), based on maximum operation between two interval sets, is given in [18], [12], and [32]. The extension to part (b) (via mathematical induction) is also so straightforward we leave it to the reader.

In this paper, we always assume that the $\vee$ operation is the maximum operation.

Observe from Theorems 1 and 2, that meet and join operations of interval sets are determined just by the two end-points of each interval set. In a type-2 FLS, the two end-points are associated with two type-1 MFs that we refer to as *upper* and *lower MFs*.

IV. Upper and Lower MFs for Type-2 FLSs

For convenience in defining the upper and lower MFs of a type-2 MF, we first give the definition of *footprint of uncertainty of a type-2 MF*.

Definition 1 (Footprint of Uncertainty of a Type-2 MF): Uncertainty in the primary membership grades of a type-2 MF consists of a bounded region that we call the *footprint of uncertainty* of a type-2 MF (e.g., see Fig. 1). It is the union of all primary membership grades.

Definition 2 (Upper and Lower MFs): An upper MF and a lower MF are two type-1 MFs that are bounds for the footprint of uncertainty of an interval type-2 MF. The upper MF is a subset that has the maximum membership grade of the footprint of uncertainty; and the lower MF is a subset that has the minimum membership grade of the footprint of uncertainty.

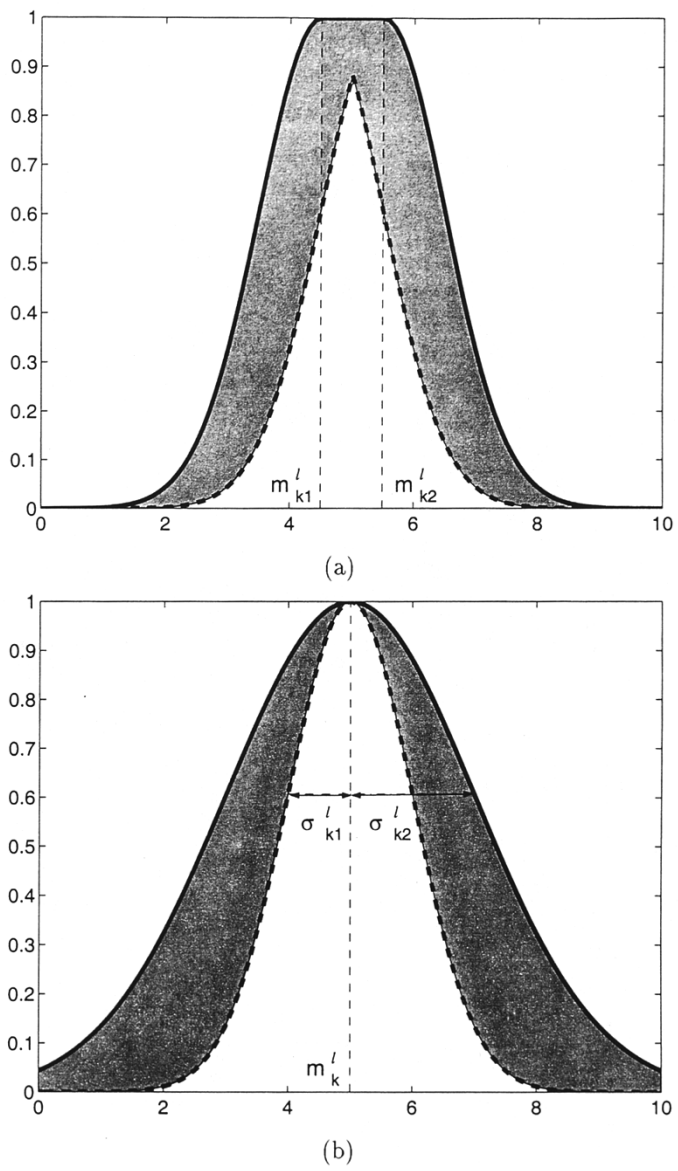

Fig. 1. The type-2 MFs for (a) Example 1 and (b) Example 2. The thick solid lines denote upper MFs and the thick dashed lines denote lower MFs. The shaded regions are the footprints of uncertainty for interval secondaries. In (a), the centers of Gaussian MFs vary from 4.5–5.5; in (b), the center of the Gaussian MFs is 5 and the variance varies from 1.0–2.0.

We use an overbar (underbar) to denote the upper (lower) MF. For example, the upper and lower MFs of $\mu_{\tilde{Q}_k^l}(x_k)$ are $\overline{\mu}_{\tilde{Q}_k^l}(x_k)$ and $\underline{\mu}_{\tilde{Q}_k^l}(x_k)$, respectively, so that

$$\mu_{\tilde{Q}_k^l}(x_k) = \int_{q^l \in [\underline{\mu}_{\tilde{Q}_k^l}(x_k), \overline{\mu}_{\tilde{Q}_k^l}(x_k)]} 1/q^l. \tag{13}$$

Similarly, we will represent $\mu_{\tilde{X}_k}(x_k)$ and $\mu_{\tilde{F}_k^l}(x_k)$ as

$$\mu_{\tilde{X}_k}(x_k) = \int_{v^l \in [\underline{\mu}_{X_k}(x_k), \overline{\mu}_{X_k}(x_k)]} 1/v^l \tag{14}$$

$$\mu_{\tilde{F}_k^l}(x_k) = \int_{w^l \in [\underline{\mu}_{F_k^l}(x_k), \overline{\mu}_{F_k^l}(x_k)]} 1/w^l \tag{15}$$

Example 1: Gaussian Primary MF with Uncertain Mean: Consider the case of a Gaussian primary MF having a fixed standard deviation σ_k^l and an uncertain mean that takes on values in $[m_{k1}^l, m_{k2}^l]$, i.e.,

$$\mu_k^l(x_k) = \exp\left[-\frac{1}{2}\left(\frac{x_k - m_k^l}{\sigma_k^l}\right)^2\right], \quad m_k^l \in [m_{k1}^l, m_{k2}^l] \tag{16}$$

where

k $1, \ldots, p$;
p number of antecedents;
l $1, \ldots, M$; and,
M number of rules.

The upper MF $\overline{\mu}_k^l(x_k)$ is [see Fig. 1(a)]

$$\overline{\mu}_k^l(x_k) = \begin{cases} \mathcal{N}(m_{k1}^l, \sigma_k^l;\ x_k), & x_k < m_{k1}^l \\ 1, & m_{k1}^l \le x_k \le m_{k2}^l \\ \mathcal{N}(m_{k2}^l, \sigma_k^l;\ x_k), & x_k > m_{k2}^l \end{cases} \tag{17}$$

where, for example

$$\mathcal{N}(m_{k1}^l, \sigma_k^l;\ x_k) \triangleq \exp\left(-\frac{1}{2}\left(\frac{x_k - m_{k1}^l}{\sigma_k^l}\right)^2\right).$$

The lower MF $\underline{\mu}_k^l(x_k)$ is [see Fig. 1(a)]

$$\underline{\mu}_k^l(x_k) = \begin{cases} \mathcal{N}(m_{k2}^l, \sigma_k^l;\ x_k), & x_k \le \dfrac{m_{k1}^l + m_{k2}^l}{2} \\ \mathcal{N}(m_{k1}^l, \sigma_k^l;\ x_k), & x_k > \dfrac{m_{k1}^l + m_{k2}^l}{2} \end{cases}. \tag{18}$$

□

From this example, we see that sometimes an upper (or a lower) MF cannot be represented by one mathematical function over its entire domain. It may consist of several branches each defined over a different segment of the entire domain. When the input is located in one domain-segment, we call its corresponding MF branch an *active branch*, e.g., in Example 1, when $x_k > ((m_{k1}^l + m_{k2}^l)/2)$, the active branch for $\underline{\mu}_k^l(x_k)$ is $\mathcal{N}(m_{k1}^l, \sigma_k^l;\ x_k)$.

When an upper (or lower) MF is represented in different segments, its left-hand and right-hand derivatives at the segment end point [e.g., $x_k = ((m_{k1}^l + m_{k2}^l)/2)$ for $\underline{\mu}_k^l(x_k)$] may not be equal, so the upper (or lower) MF may not be differentiable over the entire domain; however, it is piecewise differentiable, i.e., each branch is differentiable over its segment domain. This fact will be used by us when we tune the parameters of a type-2 FLS.

Some upper and lower MFs can be represented by one function and are differentiable over their entire domain as we demonstrate in the following example.

Example 2: Gaussian Primary MF with Uncertain Standard Deviation: Consider the case of a Gaussian primary MF having a fixed mean m_k^l and an uncertain standard deviation that takes on values in $[\sigma_{k1}^l, \sigma_{k2}^l]$, i.e.,

$$\mu_k^l(x_k) = \exp\left[-\frac{1}{2}\left(\frac{x_k - m_k^l}{\sigma_k^l}\right)^2\right], \quad \sigma_k^l \in [\sigma_{k1}^l, \sigma_{k2}^l] \tag{19}$$

where

k $1, \ldots, p$;
p number of antecedents;
l $1, \ldots, M$;
M number of rules.

The upper MF $\overline{\mu}_k^l(x_k)$ is [see Fig. 1(b)]

$$\overline{\mu}_k^l(x_k) = \mathcal{N}(m_k^l, \sigma_{k2}^l;\ x_k) \tag{20}$$

and the lower MF $\underline{\mu}_k^l(x_k)$ is [see Fig. 1(b)]

$$\underline{\mu}_k^l(x_k) = \mathcal{N}(m_k^l, \sigma_{k1}^l;\ x_k). \tag{21}$$

Note that the upper and lower membership functions are simpler for Example 2 than for Example 1. □

These examples illustrate how to define $\overline{\mu}$ and $\underline{\mu}$ so it is clear how to define these membership functions for other situations (e.g., triangular, trapezoidal, bell MFs).

V. Interval Type-2 FLSs

Our major result for interval type-2 FLSs is given in:

Theorem 3: In an interval type-2 nonsingleton FLS with type-2 fuzzification and meet under minimum or product t-norm: 1) the result of the input and antecedent operations, F^l in (9), is an interval type-1 set, i.e., $F^l = [\underline{f}^l, \overline{f}^l]$, where

$$\underline{f}^l = \sup_{\mathbf{x} \in X} \int_{X_1} \cdots \int_{X_p} \left[\underline{\mu}_{\tilde{X}_1}(x_1) \star \underline{\mu}_{\tilde{F}_1^l}(x_1)\right] \star \cdots \star \left[\underline{\mu}_{\tilde{X}_p}(x_p) \star \underline{\mu}_{\tilde{F}_p^l}(x_p)\right] \Big/ \mathbf{x} \tag{22}$$

and

$$\overline{f}^l = \sup_{\mathbf{x} \in X} \int_{X_1} \cdots \int_{X_p} \left[\overline{\mu}_{\tilde{X}_1}(x_1) \star \overline{\mu}_{\tilde{F}_1^l}(x_1)\right] \star \cdots \star \left[\overline{\mu}_{\tilde{X}_p}(x_p) \star \overline{\mu}_{\tilde{F}_p^l}(x_p)\right] \Big/ \mathbf{x} \tag{23}$$

the supremum is attained when each term in brackets attains its supremum; 2) the rule R^l fired output consequent set $\mu_{\tilde{B}^l}(y)$ in (10) is

$$\mu_{\tilde{B}^l}(y) = \int_{b^l \in [\underline{f}^l \star \underline{\mu}_{\tilde{G}^l}(y),\ \overline{f}^l \star \overline{\mu}_{\tilde{G}^l}(y)]} 1/b^l \tag{24}$$

where $\underline{\mu}_{\tilde{G}^l}(y)$ and $\overline{\mu}_{\tilde{G}^l}(y)$ are the lower and upper membership grades of $\mu_{\tilde{G}^l}(y)$; and 3) the output fuzzy set $\mu_{\tilde{B}}(y)$ in (7) is (25), as shown at the bottom of the page.

$$\mu_{\tilde{B}}(y) = \int_{b \in \left[[\underline{f}^1 \star \underline{\mu}_{\tilde{G}^1}(y)] \vee \cdots \vee [\underline{f}^N \star \underline{\mu}_{\tilde{G}^N}(y)],\ [\overline{f}^1 \star \overline{\mu}_{\tilde{G}^1}(y)] \vee \cdots \vee [\overline{f}^N \star \overline{\mu}_{\tilde{G}^N}(y)]\right]} 1/b \tag{25}$$

A. Proof of Theorem 3

1) Applying Theorem 1(a) to (5) for an interval type-2 FLS with type-2 fuzzifier and using (14) and (15), we find

$$\mu_{\tilde{Q}_k^l}(x_k) = \mu_{\tilde{X}_k}(x_k) \sqcap \mu_{\tilde{F}_k^l}(x_k) = \int_{q^l \in [\underline{\mu}_{\tilde{X}_k}(x_k) \star \underline{\mu}_{\tilde{F}_k^l}(x_k),\, \overline{\mu}_{\tilde{X}_k}(x_k) \star \overline{\mu}_{\tilde{F}_k^l}(x_k)]} 1/q^l \tag{26}$$

where $q^l = v^l \star w^l$. So, the meet between an input type-2 set and an antecedent type-2 set just involves the t-norm operation between the points in two upper or lower MFs. The upper and lower MFs of $\mu_{\tilde{Q}_k^l}(x_k)$ are

$$\overline{\mu}_{\tilde{Q}_k^l}(x_k) = \int_{X_k} \left[\overline{\mu}_{\tilde{X}_k}(x_k) \star \overline{\mu}_{\tilde{F}_k^l}(x_k)\right] \Big/ x_k \tag{27}$$

$$\underline{\mu}_{\tilde{Q}_k^l}(x_k) = \int_{X_k} \left[\underline{\mu}_{\tilde{X}_k}(x_k) \star \underline{\mu}_{\tilde{F}_k^l}(x_k)\right] \Big/ x_k. \tag{28}$$

The meet operations in (8) are in a p-dimensional Cartesian product space so the meet operation is over all points $x_k \in X_k, k = 1, \ldots, p$. Based on Theorem 1(b), we know that the upper membership grades of $\mu_{\tilde{Q}^l}(\mathbf{x})$, $\overline{\mu}_{\tilde{Q}^l}(\mathbf{x})$ (a type-1 MF) are obtained from the t-norm of membership grades in $\overline{\mu}_{\tilde{Q}_k^l}(x_k^l)$; hence, from (27), we find

$$\overline{\mu}_{\tilde{Q}^l}(\mathbf{x}) = \int_{X_1} \cdots \int_{X_p} \left[\overline{\mu}_{\tilde{X}^1}(x_1) \star \overline{\mu}_{\tilde{F}_1^l}(x_1)\right] \star \cdots \star \left[\overline{\mu}_{\tilde{X}^p}(x_p) \star \overline{\mu}_{\tilde{F}_p^l}(x_p)\right] \Big/ \mathbf{x}. \tag{29}$$

The lower membership grades $\underline{\mu}_{\tilde{Q}^l}(\mathbf{x})$ (a type-1 MF), are the t-norm of the membership grades in $\underline{\mu}_{\tilde{Q}_k^l}(x_k^l)$; hence, from (28) we find

$$\underline{\mu}_{\tilde{Q}^l}(\mathbf{x}) = \int_{X_1} \cdots \int_{X_p} \left[\underline{\mu}_{\tilde{X}^1}(x_1) \star \underline{\mu}_{\tilde{F}_1^l}(x_1)\right] \star \cdots \star \left[\underline{\mu}_{\tilde{X}^p}(x_p) \star \underline{\mu}_{\tilde{F}_p^l}(x_p)\right] \Big/ \mathbf{x}. \tag{30}$$

The *join* operation in (9) is over all points $\mathbf{x}$ in X. Based on Theorem 2, we know that the right-most point of the join of n ($n \geq 2$) interval sets is the maximum value of all the right-most points in the n interval sets; so, the right-most point $\overline{f}^l$ of F^l comes from the maximum value (supremum) of $\overline{\mu}_{\tilde{Q}^l}(\mathbf{x})$ (the right-most point of interval set $\mu_{\tilde{Q}^l}(\mathbf{x}')$ for each value of $\mathbf{x}'$); hence, from (29) we find

$$\overline{f}^l = \sup_{\mathbf{x} \in X} \int_{X_1} \cdots \int_{X_p} \left[\overline{\mu}_{\tilde{X}^1}(x_1) \star \overline{\mu}_{\tilde{F}_1^l}(x_1)\right] \star \cdots \star \left[\overline{\mu}_{\tilde{X}^p}(x_p) \star \overline{\mu}_{\tilde{F}_p^l}(x_p)\right] \Big/ \mathbf{x}. \tag{31}$$

Similarly, the left-most point $\underline{f}^l$ of F^l comes from the maximum value (supremum) of $\underline{\mu}_{\tilde{Q}^l}(\mathbf{x})$; hence, from (30) we find

$$\underline{f}^l = \sup_{\mathbf{x} \in X} \int_{X_1} \cdots \int_{X_p} \left[\underline{\mu}_{\tilde{X}^1}(x_1) \star \underline{\mu}_{\tilde{F}_1^l}(x_1)\right] \star \cdots \star \left[\underline{\mu}_{\tilde{X}^p}(x_p) \star \underline{\mu}_{\tilde{F}_p^l}(x_p)\right] \Big/ \mathbf{x}. \tag{32}$$

The suprema in (31) and (32) are, overall, $\mathbf{x}$ in X. By the monotonicity property of a t-norm [42], [27], the supremum is attained when each term in brackets attains its supremum.

2) Based on (9), (31), (32), and Theorem 2(a), we evaluate (10) as

$$\mu_{\tilde{B}^l}(y) = \mu_{\tilde{G}^l}(y) \sqcap F^l = \mu_{\tilde{G}^l}(y) \sqcap \int_{f^l \in [\underline{f}^l, \overline{f}^l]} 1/f^l = \int_{b^l \in [\underline{f}^l \star \underline{\mu}_{\tilde{G}^l}(y),\, \overline{f}^l \star \overline{\mu}_{\tilde{G}^l}(y)]} 1/b^l. \tag{33}$$

3) Because $\mu_{\tilde{B}^l}(y)$ ($l = 1, \ldots, N$) are interval sets, it is straightforward to obtain $\mu_{\tilde{B}}(y)$ in (7) using Theorem 2(b). The result is (25).

□

In evaluating (22) and (23), the supremum is attained when each term in brackets attains its supremum; so, in the inference of a type-2 FLS, we will examine

$$\overline{f}_k^l \triangleq \sup_{x_k \in X_k} \int_{X_k} \left[\overline{\mu}_{\tilde{X}_k}(x_k) \star \overline{\mu}_{\tilde{F}_k^l}(x_k)\right] \Big/ x_k \tag{34}$$

$$\underline{f}_k^l \triangleq \sup_{x_k \in X_k} \int_{X_k} \left[\underline{\mu}_{\tilde{X}_k}(x_k) \star \underline{\mu}_{\tilde{F}_k^l}(x_k)\right] \Big/ x_k \tag{35}$$

where $k = 1, \ldots, p$, and $\star$ is a t-norm; then, $\overline{f}^l$ and $\underline{f}^l$ can be re-expressed as

$$\overline{f}^l = \mathcal{T}_{k=1}^p \overline{f}_k^l \tag{36}$$

$$\underline{f}^l = \mathcal{T}_{k=1}^p \underline{f}_k^l \tag{37}$$

where $\mathcal{T}$ denotes t-norm. We illustrate (36) and (37) below in Section V-C.

B. Corollaries to Theorem 3

When the input is fuzzified to a type-1 fuzzy set so that $\mu_{\tilde{X}_k} \rightarrow \mu_{X_k}$ ($k = 1, \ldots, p$), the upper and lower MFs of $\mu_{\tilde{X}_k}$ merge into one MF $\mu_{X_k}(x_k)$ in which case Theorem 3 simplifies to the following.

Corollary 1: In an interval type-2 FLS with *nonsingleton type-1 fuzzification* and meet under minimum or product t-norm, $\underline{f}^l$ and $\overline{f}^l$ in (22) and (23) simplify to

$$\underline{f}^l = \sup_{\mathbf{x} \in X} \int_{X_1} \cdots \int_{X_p} \left[\mu_{X_1}(x_1) \star \underline{\mu}_{\tilde{F}_1^l}(x_1)\right] \star \cdots \star \left[\mu_{X_p}(x_p) \star \underline{\mu}_{\tilde{F}_p^l}(x_p)\right] \Big/ \mathbf{x} \tag{38}$$

and

$$\overline{f}^l = \sup_{\mathbf{x} \in X} \int_{X_1} \cdots \int_{X_p} \left[\mu_{X_1}(x_1) \star \overline{\mu}_{\tilde{F}_1^l}(x_1)\right] \star \cdots \star \left[\mu_{X_p}(x_p) \star \overline{\mu}_{\tilde{F}_p^l}(x_p)\right] \Big/ \mathbf{x} \tag{39}$$

where μ_{X_k} ($k = 1, \ldots, p$) is the type-1 fuzzified input.

When a singleton fuzzifier is used, the upper and lower MFs of $\mu_{\tilde{X}_k}(x_k)$ merge into one crisp value, namely one, in which case Theorem 3 simplifies further to the following.

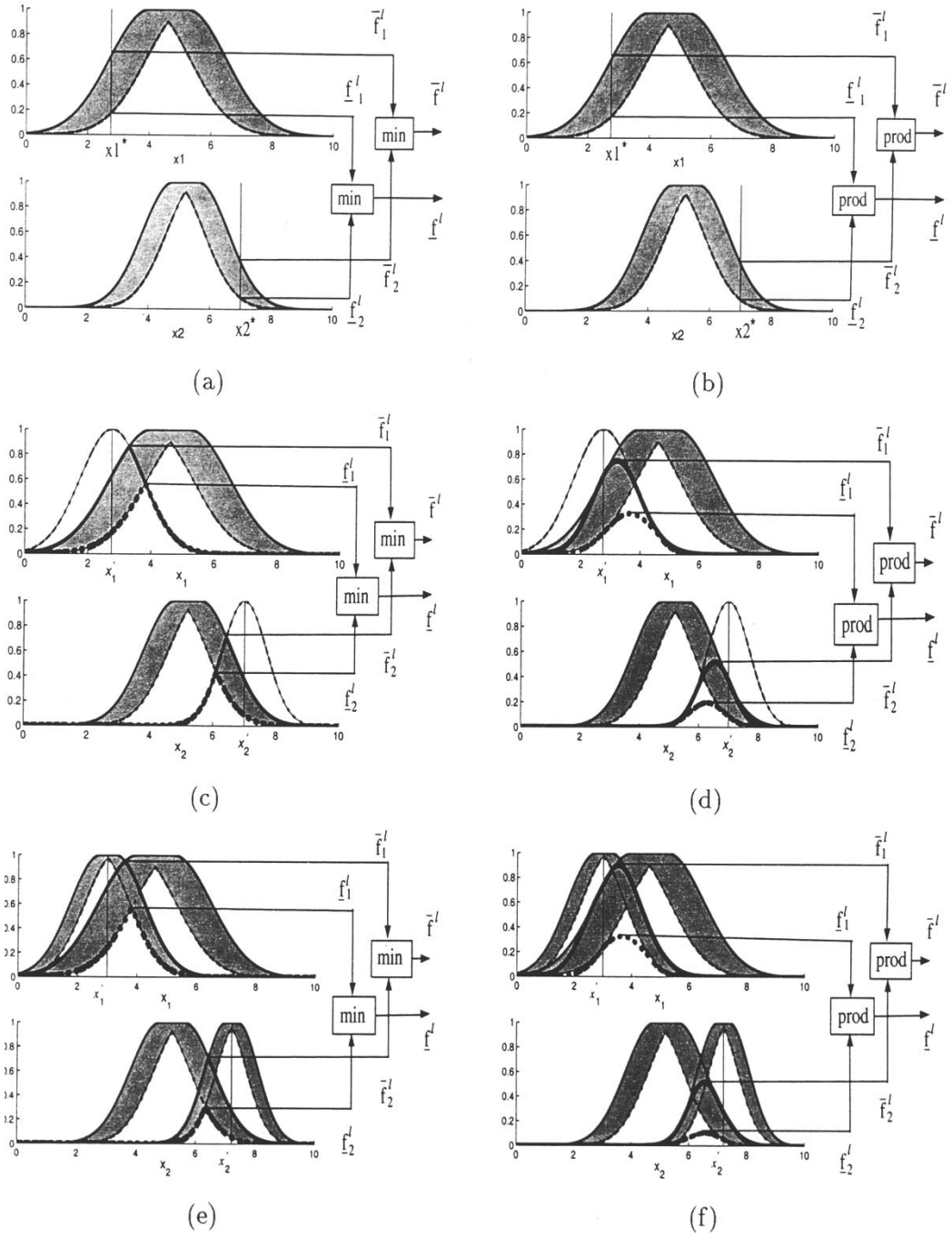

Fig. 2. Type-2 FLS: input and antecedent operations. (a) Singleton fuzzification with minimum t-norm; (b) singleton fuzzification with product t-norm; (c) NS type-1 fuzzification with minimum t-norm; (d) NS type-1 fuzzification with product t-norm; (e) NS type-2 fuzzification with minimum t-norm; and (f) NS type-2 fuzzification with product t-norm. The dark shaded regions depict the meet between input and antecedent [computed using Theorem 1(a)].

Corollary 2: In an interval type-2 FLS with *singleton fuzzification* and meet under minimum or product t-norm $\underline{f}^l$ and $\overline{f}^l$ in (22) and (23) simplify to

$$\underline{f}^l = \underline{\mu}_{\tilde{F}_1^l}(x_1) \star \cdots \star \underline{\mu}_{\tilde{F}_p^l}(x_p) \tag{40}$$

and

$$\overline{f}^l = \overline{\mu}_{\tilde{F}_1^l}(x_1) \star \cdots \star \overline{\mu}_{\tilde{F}_p^l}(x_p) \tag{41}$$

where x_i $(i = 1, \ldots, p)$ denotes the location of the singleton.

The proofs of these corollaries are so simple, we leave them for the reader.

C. Illustrative Examples

Example 3—Pictorial Representation of Input and Antecedent Operations: In Fig. 2, we plot the results of input and antecedent operations with singleton, type-1 nonsingleton, and type-2 nonsingleton fuzzifications. The number of antecedents is $p = 2$. In all cases, the firing stength is an interval type-1 set, $[\underline{f}^l, \overline{f}^l]$, where $\underline{f}^l = \underline{f}_1^l \star \underline{f}_2^l$ and $\overline{f}^l = \overline{f}_1^l \star \overline{f}_2^l$. For singleton fuzzification [Fig. 2(a) and (b)], $\overline{f}_k^l$ denotes the firing strength between input x_k and $\overline{\mu}_{\tilde{F}_l^k}$, namely $\overline{\mu}_{\tilde{F}_l^k}(x_k)$; and $\underline{f}_k^l$ denotes the firing strength between input x_k and $\underline{\mu}_{\tilde{F}_l^k}$,

TABLE I
$\overline{x}^l_{k,\max}$ FOR EXAMPLE 4

Cases	$m_{\tilde{X}_k}$ locations	product t-norm	minimum t-norm
1 (Fig. 5a)	$m_{\tilde{X}_k} \le m_{\tilde{F}^i_{k1}}$	$\overline{x}^l_{k,\max} = \frac{\sigma^2_{\tilde{X}_{k2}} m_{\tilde{F}^i_{k1}} + \sigma^2_{\tilde{F}^i_k} m_{\tilde{X}_k}}{\sigma^2_{\tilde{X}_{k2}} + \sigma^2_{\tilde{F}^i_k}}$	$\overline{x}^l_{k,\max} = \frac{\sigma_{\tilde{X}_{k2}} m_{\tilde{F}^i_{k1}} + \sigma_{\tilde{F}^i_k} m_{\tilde{X}_k}}{\sigma_{\tilde{X}_{k2}} + \sigma_{\tilde{F}^i_k}}$
2 (Figs. 5b,c,d)	$m_{\tilde{X}_k} \in [m_{\tilde{F}^i_{k1}}, m_{\tilde{F}^i_{k2}}]$	$\overline{x}^l_{k,\max} = m_{\tilde{X}_k}$	$\overline{x}^l_{k,\max} = m_{\tilde{X}_k}$
3 (Fig. 5e)	$m_{\tilde{X}_k} \ge m_{\tilde{F}^i_{k2}}$	$\overline{x}^l_{k,\max} = \frac{\sigma^2_{\tilde{X}_{k2}} m_{\tilde{F}^i_{k2}} + \sigma^2_{\tilde{F}^i_k} m_{\tilde{X}_k}}{\sigma^2_{\tilde{X}_{k2}} + \sigma^2_{\tilde{F}^i_k}}$	$\overline{x}^l_{k,\max} = \frac{\sigma_{\tilde{X}_{k2}} m_{\tilde{F}^i_{k2}} + \sigma_{\tilde{F}^i_k} m_{\tilde{X}_k}}{\sigma_{\tilde{X}_{k2}} + \sigma_{\tilde{F}^i_k}}$

TABLE II
$\underline{x}^l_{k,\max}$ FOR EXAMPLE 4 BASED ON PRODUCT t-NORM

Cases	$m_{\tilde{X}_k}$ locations	product t-norm
1 (Figs. 5a,b)	$m_{\tilde{X}_k} < \frac{m_{\tilde{F}^i_{k1}} + m_{\tilde{F}^i_{k2}}}{2} - \frac{\sigma^2_{\tilde{X}_{k1}} (m_{\tilde{F}^i_{k2}} - m_{\tilde{F}^i_{k1}})}{2\sigma^2_{\tilde{F}^i_k}}$	$\underline{x}^l_{k,\max} = \frac{\sigma^2_{\tilde{X}_{k1}} m_{\tilde{F}^i_{k2}} + \sigma^2_{\tilde{F}^i_k} m_{\tilde{X}_k}}{\sigma^2_{\tilde{X}_{k1}} + \sigma^2_{\tilde{F}^i_k}}$
2 (Fig. 5c)	$m_{\tilde{X}_k} \in \left[\frac{m_{\tilde{F}^i_{k1}} + m_{\tilde{F}^i_{k2}}}{2} - \frac{\sigma^2_{\tilde{X}_{k1}} (m_{\tilde{F}^i_{k2}} - m_{\tilde{F}^i_{k1}})}{2\sigma^2_{\tilde{F}^i_k}}, \frac{m_{\tilde{F}^i_{k1}} + m_{\tilde{F}^i_{k2}}}{2} + \frac{\sigma^2_{\tilde{X}_{k1}} (m_{\tilde{F}^i_{k2}} - m_{\tilde{F}^i_{k1}})}{2\sigma^2_{\tilde{F}^i_k}}\right]$	$\underline{x}^l_{k,\max} = \frac{m_{\tilde{F}^i_{k1}} + m_{\tilde{F}^i_{k2}}}{2}$
3 (Figs. 5d,e)	$m_{\tilde{X}_k} > \frac{m_{\tilde{F}^i_{k1}} + m_{\tilde{F}^i_{k2}}}{2} + \frac{\sigma^2_{\tilde{X}_{k1}} (m_{\tilde{F}^i_{k2}} - m_{\tilde{F}^i_{k1}})}{2\sigma^2_{\tilde{F}^i_k}}$	$\underline{x}^l_{k,\max} = \frac{\sigma^2_{\tilde{X}_{k1}} m_{\tilde{F}^i_{k1}} + \sigma^2_{\tilde{F}^i_k} m_{\tilde{X}_k}}{\sigma^2_{\tilde{X}_{k1}} + \sigma^2_{\tilde{F}^i_k}}$

namely $\underline{\mu}_{\tilde{F}^k_l}(x_k)$, $(k = 1, 2)$, as established by Corollary 2. For nonsingleton type-1 fuzzification [Fig. 2(c) and (d)], $\overline{f}^l_k$ denotes the supremum of the firing strength between the t-norm of membership functions μ_{X_k} and $\overline{\mu}_{\tilde{F}^k_l}$; and $\underline{f}^l_k$ denotes the supremum of the firing strength between the t-norm of membership functions μ_{X_k} and $\underline{\mu}_{\tilde{F}^k_l}$, $(k = 1, 2)$, as established by Corollary 1. For nonsingleton type-2 fuzzification [Fig. 2(e) and (f)], $\overline{f}^l_k$ denotes the supremum of the firing strength between the t-norm of upper membership functions $\overline{\mu}_{\tilde{X}_k}$ and $\overline{\mu}_{\tilde{F}^k_l}$; and, $\underline{f}^l_k$ denotes the supremum of the firing strength between the t-norm of lower membership functions $\underline{\mu}_{\tilde{X}_k}$ and $\underline{\mu}_{\tilde{F}^k_l}$, $(k = 1, 2)$, as established by Theorem 3. The main thing to observe from these figures is that regardless of singleton or nonsingleton fuzzification and minimum or product t-norm, the result of input and antecedent operations is an interval type-1 set that is determined by its left-most point $\underline{f}^l$ and right-most point $\overline{f}^l$.

Example 4—Input is a Gaussian Primary MF with Uncertain Standard Deviation and Antecedents are Gaussian Primary MFs with Uncertain Means: In this example, we compute $\overline{f}^l_k$ and $\underline{f}^l_k$ when a Gaussian primary MF with an uncertain standard deviation (as in Example 2) is used as input fuzzy sets and Gaussian primary MFs with uncertain means (as in Example 1) are used as antecedent MFs. This case is important to our time-series forecasting application in Section VIII. In this case

$$\mu_{\tilde{X}_k}(x_k) = \exp\left[-\frac{1}{2}\left(\frac{x_k - m_{\tilde{X}_k}}{\sigma_{X_k}}\right)^2\right] \qquad \sigma_{X_k} \in [\sigma_{X_{k1}}, \sigma_{X_{k2}}] \tag{42}$$

and its upper and lower MFs $\overline{\mu}_{\tilde{X}_k}(x_k)$ and $\underline{\mu}_{\tilde{X}_k}(x_k)$ are obtained from (20) and (21), respectively, by replacing m^l_k by $m_{\tilde{X}_k}$, σ^l_{k1} by $\sigma_{\tilde{X}_{k1}}$, and σ^l_{k2} by $\sigma_{\tilde{X}_{k2}}$. The kth antecedent MF has the following form:

$$\mu_{\tilde{F}^l_k}(x_k) = \exp\left[-\frac{1}{2}\left(\frac{x_k - m_{\tilde{F}^i_k}}{\sigma_{\tilde{F}^i_k}}\right)^2\right] \qquad m_{\tilde{F}^i_k} \in [m_{\tilde{F}^i_{k1}}, m_{\tilde{F}^i_{k2}}] \tag{43}$$

and its upper and lower MFs $\overline{\mu}_{\tilde{F}^l_k}(x_k)$ and $\underline{\mu}_{\tilde{F}^l_k}(x_k)$ are obtained from (17) and (18), respectively, by replacing m^l_{k1} by $m_{\tilde{F}^i_{k1}}$, m^l_{k2} by $m_{\tilde{F}^i_{k2}}$ and σ^l_k by $\sigma_{\tilde{F}^i_k}$. Observe that there are six parameters that determine these two type-2 Gaussian MFs: $m_{\tilde{F}^i_{k1}}$, $m_{\tilde{F}^i_{k2}}$, $\sigma_{\tilde{F}^i_k}$, $m_{\tilde{X}_k}$, $\sigma_{\tilde{X}_{k1}}$, and $\sigma_{\tilde{X}_{k2}}$. In this example, as in [27], we assume that

$$\sigma_{\tilde{F}^i_k} \ge \sigma_{\tilde{X}_{k2}} \tag{44}$$

and our objective is to evaluate (34) and (35). Equation (44) means that uncertainty in each input set is always no more than the uncertainty in the antecedent.

We denote the value of x_k at which the supremum of (34) occurs as $\overline{x}^l_{k,\max}$ and the value of x_k at which the supremum of (35) occurs as $\underline{x}^l_{k,\max}$. The results for $\overline{x}^l_{k,\max}$ and $\underline{x}^l_{k,\max}$ of this example are carried out in Appendix A, and are summarized in Tables I–III. From these results, it is straightforward to compute $\overline{f}^l_k$ and $\underline{f}^l_k$ using (34) and (35), i.e.,

$$\overline{f}^l_k = \overline{\mu}_{\tilde{X}_k}(\overline{x}^l_{k,\max}) \star \overline{\mu}_{\tilde{F}^l_k}(\overline{x}^l_{k,\max}) \tag{45}$$

$$\underline{f}^l_k = \underline{\mu}_{\tilde{X}_k}(\underline{x}^l_{k,\max}) \star \underline{\mu}_{\tilde{F}^l_k}(\underline{x}^l_{k,\max}). \tag{46}$$

When the input is fuzzified to a type-1 Gaussian MF, then $\sigma_{\tilde{X}_{k1}} = \sigma_{\tilde{X}_{k2}}$, and we can easily obtain $\overline{x}^l_{k,\max}$ and $\underline{x}^l_{k,\max}$ based on Tables I–III. When a singleton fuzzifier is used, the

TABLE III
$\underline{x}^l_{k,\max}$ FOR EXAMPLE 4 BASED ON MINIMUM t-NORM

Cases	$m_{\tilde{X}_k}$ locations	minimum t-norm
1 (Figs. 5a,b)	$m_{\tilde{X}_k} < \frac{m_{\tilde{F}^i_{k1}}+m_{\tilde{F}^i_{k2}}}{2} - \frac{\sigma_{\tilde{X}_{k1}}(m_{\tilde{F}^i_{k2}}-m_{\tilde{F}^i_{k1}})}{2\sigma_{\tilde{F}^i_k}}$	$\underline{x}^l_{k,\max} = \frac{\sigma_{\tilde{X}_{k1}} m_{\tilde{F}^i_{k1}} + \sigma_{\tilde{F}^i_k} m_{\tilde{X}_k}}{\sigma_{\tilde{X}_{k1}}+\sigma_{\tilde{F}^i_k}}$
2 (Fig. 5c)	$m_{\tilde{X}_k} \in \left[\frac{m_{\tilde{F}^i_{k1}}+m_{\tilde{F}^i_{k2}}}{2} - \frac{\sigma_{\tilde{X}_{k1}}(m_{\tilde{F}^i_{k2}}-m_{\tilde{F}^i_{k1}})}{2\sigma_{\tilde{F}^i_k}}, \frac{m_{\tilde{F}^i_{k1}}+m_{\tilde{F}^i_{k2}}}{2} + \frac{\sigma_{\tilde{X}_{k1}}(m_{\tilde{F}^i_{k2}}-m_{\tilde{F}^i_{k1}})}{2\sigma_{\tilde{F}^i_k}}\right]$	$\underline{x}^l_{k,\max} = \frac{m_{\tilde{F}^i_{k1}}+m_{\tilde{F}^i_{k2}}}{2}$
3 (Figs. 5d,e)	$m_{\tilde{X}_k} > \frac{m_{\tilde{F}^i_{k1}}+m_{\tilde{F}^i_{k2}}}{2} + \frac{\sigma_{\tilde{X}_{k1}}(m_{\tilde{F}^i_{k2}}-m_{\tilde{F}^i_{k1}})}{2\sigma_{\tilde{F}^i_k}}$	$\underline{x}^l_{k,\max} = \frac{\sigma_{\tilde{X}_{k1}} m_{\tilde{F}^i_{k1}} + \sigma_{\tilde{F}^i_k} m_{\tilde{X}_k}}{\sigma_{\tilde{X}_{k1}}+\sigma_{\tilde{F}^i_k}}$

results in Tables I–III simplify even further since $\underline{x}^l_{k,\max} = \overline{x}^l_{k,\max} = x_k$.

VI. TYPE REDUCTION AND DEFUZZIFICATION

A type-2 FLS is a mapping f: $\mathcal{R}^p \to \mathcal{R}^1$. After fuzzification, fuzzy inference, type-reduction, and defuzzification, we obtain a crisp output. For an interval type-2 FLS, this crisp output is the center of the type-reduced set. Based on Theorem 3 and Corollaries 1 and 2, we know that for an interval type-2 FLS, regardless of singleton or nonsingleton fuzzification and minimum or product t-norm, the result of input and antecedent operations (firing strength) is an interval type-1 set, which is determined by its left-most and right-most points $\underline{f}^l$ and $\overline{f}^l$ (e.g., see Fig. 2). The fired output consequent set $\mu_{\tilde{B}^l}(y)$ of rule R^l can be obtained from the fired interval strength using (24) or Corollaries 1 or 2 and (24). Then the fired combined output consequent set $\mu_{\tilde{B}}(y)$ can be computed using (25).

Type-reduction was proposed by Karnik and Mendel [11], [12], [17]. It is an "extended version" [using the extension principle [41] of type-1 defuzzification methods and is called type-reduction because this operation takes us from the type-2 output sets of the FLS to a type-1 set that is called the "type-reduced set." This set may then be defuzzified to obtain a single crisp number; however, in many applications, the type reduced set may be more important than a single crisp number since it conveys a measure of uncertainties that have flown through the type-2 FLS.

There exist many kinds of type-reduction, such as centroid, center-of-sets, height, and modified height, the details of which are given in [11], [12], and [17]. In this paper, for illustrative purposes, we focus on center-of-sets type-reduction, which can be expressed as

$$Y_{\cos}(Y^1, \ldots, Y^M, F^1, \ldots, F^M) = [y_l, y_r] = \int_{y^1} \cdots \int_{y^M} \int_{f^1} \cdots \int_{f^M} 1 \Big/ \frac{\sum_{i=1}^{M} f^i y^i}{\sum_{i=1}^{M} f^i} \quad (47)$$

where

$Y_{\cos}$	interval set determined by two end points y_l and y_r;
$f^i \in F^i$	$[\underline{f}^i, \overline{f}^i]$;
$y^i \in Y^i = [y^i_l, y^i_r]$ and Y^i	centroid of the type-2 interval consequent set $\tilde{G}^i$ (the centroid of a type-2 fuzzy set is described in [11], [16], and [12]);
i	$1, \ldots, M$.

Observe, that each set on the right-hand side (RHS) of (47) is an interval type-1 set, hence, $Y_{\cos}(Y^1, \ldots, Y^M, F^1, \ldots, F^M)$ is also an interval type-1 set. So, to find $Y_{\cos}(Y^1, \ldots, Y^M, F^1, \ldots, F^M)$, we just need to compute the two end-points of this interval. Unfortunately, no closed-form formula is available for $Y_{\cos}$.

For any value $y \in Y_{\cos}$, y can be represented as

$$y = \frac{\sum_{i=1}^{M} f^i y^i}{\sum_{i=1}^{M} f^i} \quad (48)$$

the maximum value of y is y_r and the minimum value of y is y_l. From (48), we see that y is a monotonic increasing function with respect to y^i; so y_r is associated only with y^i_r and, similarly, y_l is associated only with y^i_l. In the center of sets (COS)-type-reduction method, Karnik and Mendel [12], [17] have shown that the two end points of $Y_{\cos}$, y_r, and y_l depend only on a mixture of $\overline{f}^i$ or $\underline{f}^i$ values, since $f^i \in F^i = [\underline{f}^i, \overline{f}^i]$. In this case, y_l and y_r can each be represented as a fuzzy basis function (FBF) expansion, i.e.,

$$y_l = \frac{\sum_{i=1}^{M} f^i_l y^i_l}{\sum_{i=1}^{M} f^i_l} = \sum_{i=1}^{M} y^i_l p^i_l \quad (49)$$

where f^i_l denotes the firing strength membership grade [either $\underline{f}^i$ or $\overline{f}^i$] contributing to the left-most point y_l and $p^i_l = f^i_l / \sum_{i=1}^{M} f^i_l$ is the FBF. Similarly

$$y_r = \frac{\sum_{i=1}^{M} f^i_r y^i_r}{\sum_{i=1}^{M} f^i_r} = \sum_{i=1}^{M} y^i_r p^i_r \quad (50)$$

where $\underline{f}_r^i$ denotes the firing strength membership grade (either $\underline{f}^i$ or $\overline{f}^i$) contributing to the right-most point y_r and $p_r^i = f_r^i / \sum_{i=1}^{M} f_r^i$ is another FBF.

Note that whereas a type-1 FLS is characterized by a single FBF expansion [22], [37], an interval type-2 FLS is characterized by two FBF expansions. A general type-2 FLS is characterized by a huge number of FBF expansions [12], [17]; hence, we have demonstrated that by choosing secondary membership functions to be interval sets, the complexity of a general type-2 FLS is vastly reduced.

In order to compute y_l and y_r, we need to compute $\{f_l^i, i = 1, 2, \ldots, M\}$ and $\{f_r^i, i = 1, 2, \ldots, M\}$. This can be done using the exact computational procedure given in [12], [16], and [17]. Here, we briefly provide the computation procedure for y_r. Without loss of generality, assume the y_r^is are arranged in ascending order, i.e., $y_r^1 \le y_r^2 \le \ldots \le y_r^M$.

1) Compute y_r in (50) by initially setting $f_r^i = ((\overline{f}^i + \underline{f}^i)/2)$ for $i = 1, \ldots, M$, where $\overline{f}^i$ and $\underline{f}^i$ have been previously computed using (22) and (23) and let $y_r' \triangleq y_r$.
2) Find R ($1 \le R \le M-1$) such that $y_r^R \le y_r' \le y_r^{R+1}$.
3) Compute y_r in (50) with $f_r^i = \underline{f}^i$ for $i \le R$ and $f_r^i = \overline{f}^i$ for $i > R$ and let $y_r'' \triangleq y_r$.
4) If $y_r'' \ne y_r'$, then go to Step 5). If $y_r'' = y_r'$, then stop and set $y_r \triangleq y_r''$.
5) Set y_r' equal to y_r'' and return to Step 2).

This four-step computation procedure [Step 1) is an initialization step] has been proven to converge to the exact solution in no more than M iterations [12]. Observe that in this procedure, the number R is very important. For $i \le R$, $f_r^i = \underline{f}^i$, and for $i > R$, $f_r^i = \overline{f}^i$; so y_r can be represented as

$$y_r = y_r\left(\underline{f}^1, \ldots, \underline{f}^R, \overline{f}^{R+1}, \ldots, \overline{f}^M, y_r^1, \ldots, y_r^M\right). \quad (51)$$

The procedure for computing y_l is very similar. Just replace y_r^i by y_l^i and, in Step 2), find L ($1 \le L \le M-1$) such that $y_l^L \le y_l' \le y_l^{L+1}$ and, in step 3, let $f_l^i = \overline{f}^i$ for $i \le L$, and $f_l^i = \underline{f}^i$ for $i > L$. Then y_l can be represented as

$$y_l = y_l\left(\overline{f}^1, \ldots, \overline{f}^L, \underline{f}^{L+1}, \ldots, \underline{f}^M, y_l^1, \ldots, y_l^M\right). \quad (52)$$

Because $Y_{\cos}$ is an interval set, we defuzzify it using the average of y_l and y_r; hence, the defuzzified output of an interval type-2 FLS is

$$f(\mathbf{x}) = \frac{y_l + y_r}{2}. \quad (53)$$

A perfect FLS should have $f(\mathbf{x}) = d$, where d is the desired output but, generally, there exist errors between the desired output and actual output. We, therefore, need a design procedure for tuning the parameters of the FLS in order to minimize such errors.

VII. Designing Interval Type-2 FLSs Based on Tuning

Given an input–output training pair $(\mathbf{x}, d)$, $\mathbf{x} \in R^p$ and $d \in R$, we wish to design an interval type-2 FLS with output (53) so that the error function

$$e = \tfrac{1}{2}[f(\mathbf{x}) - d]^2 \quad (54)$$

is minimized. Based on the analysis in Section VI, we know that only the upper and lower MFs and the two endpoints of Y^i (the center of the consequent set) determine $f(\mathbf{x})$. So we want to tune the upper and lower MFs and the consequent parameters $Y^i = [y_l^i, y_r^i]$. Since an interval type-2 FLS can be characterized by two FBF expansions that generate the points y_l and y_r, respectively, we can focus on tuning the parameters of just these two type-1 FLSs.

Given T input–output training samples $(\mathbf{x}^t, d^t)$, $(t = 1, \ldots, T)$, we wish to update the design parameters so that (54) is minimized for E training epochs (updating the parameters using all the T training samples one time is called "one epoch"). A general method for doing this is as follows.

1) Initialize all the parameters including the parameters in antecedent and consequent MFs and input sets.
2) Set the counter of training epoch $e \triangleq 0$.
3) Set the counter of training data sample $t \triangleq 1$.
4) Apply $p \times 1$ input $\mathbf{x}^t$ to the type-2 FLS, and compute the total firing degree for each rule, i.e., compute $\overline{f}^i$ and $\underline{f}^i$ $(i = 1, 2, \ldots, p)$ using Theorem 3.
5) Compute y_l and y_r, as described in Section VI (which leads to a reordering of the M rules; but, they are then renumbered 1, 2, …, M). This will establish L and R, so that y_l and y_r can be expressed as

$$\begin{aligned} y_l &= y_l\left(\overline{f}^1, \ldots, \overline{f}^L, \underline{f}^{L+1}, \ldots, \underline{f}^M, y_l^1, \ldots, y_l^M\right) \\ &= \frac{\sum_{i=1}^{L} \overline{f}^i y_l^i + \sum_{j=L+1}^{M} \underline{f}^j y_l^j}{\sum_{i=1}^{L} \overline{f}^i + \sum_{j=L+1}^{M} \underline{f}^j} \end{aligned} \quad (55)$$

$$\begin{aligned} y_r &= y_r\left(\underline{f}^1, \ldots, \underline{f}^R, \overline{f}^{R+1}, \ldots, \overline{f}^M, y_r^1, \ldots, y_r^M\right) \\ &= \frac{\sum_{i=1}^{R} \underline{f}^i y_r^i + \sum_{j=R+1}^{M} \overline{f}^j y_r^j}{\sum_{i=1}^{R} \underline{f}^i + \sum_{j=R+1}^{M} \overline{f}^j}. \end{aligned} \quad (56)$$

6) Compute $f(\mathbf{x}^t) = (y_l + y_r)/2$, which is the defuzzified output of the type-2 FLS.
7) Determine the explicit dependence of y_l and y_r on membership functions (because L and R obtained in Step 5) may have changed from one iteration to the next, the dependence of y_l and y_r on MFs may also have changed). To do this, first determine the dependence of $\underline{f}^i$ and $\overline{f}^i$ on membership functions, using (34)–(37), i.e., $\underline{f}^i$ is determined by $\underline{f}_1^i(\underline{\mu}_{\tilde{X}_1}(x_1), \underline{\mu}_{\tilde{F}_1^i}(x_1))$, …,

$\underline{f}_p^i(\underline{\mu}_{\tilde{X}^p}(x_p),\ \underline{\mu}_{\tilde{F}_p^i}(x_p))$, and, $\overline{f}^i$ is determined by $\overline{f}_1^i(\overline{\mu}_{\tilde{X}^1}(x_1),\ \overline{\mu}_{\tilde{F}_1^i}(x_1)),\ \ldots,\ \overline{f}_p^i(\overline{\mu}_{\tilde{X}^p}(x_p),\ \overline{\mu}_{\tilde{F}_p^i}(x_p))$. Consequently

$$\begin{aligned} y_l =& y_l\Big(\overline{\mu}_{\tilde{X}^1}(x_1), \overline{\mu}_{\tilde{F}_1^1}(x_1), \ldots, \overline{\mu}_{\tilde{X}^p}(x_p), \overline{\mu}_{\tilde{F}_p^1}(x_p), \\ & \ldots, \overline{\mu}_{\tilde{X}^1}(x_1), \overline{\mu}_{\tilde{F}_1^L}(x_1), \ldots, \overline{\mu}_{\tilde{X}^p}(x_p), \overline{\mu}_{\tilde{F}_p^L}(x_p), \\ & \underline{\mu}_{\tilde{X}^1}(x_1), \underline{\mu}_{\tilde{F}_1^{L+1}}(x_1), \ldots, \underline{\mu}_{\tilde{X}^p}(x_p), \underline{\mu}_{\tilde{F}_p^{L+1}}(x_p), \\ & \ldots, \underline{\mu}_{\tilde{X}^1}(x_1), \underline{\mu}_{\tilde{F}_1^M}(x_1), \ldots, \underline{\mu}_{\tilde{X}^p}(x_p), \\ & \underline{\mu}_{\tilde{F}_p^M}(x_p), y_l^1, \ldots, y_l^M\Big) \\ =& y_l\Big(\overline{\mu}_{\tilde{X}^1}(x_1), \ldots, \overline{\mu}_{\tilde{X}^p}(x_p), \underline{\mu}_{\tilde{X}^1}(x_1), \ldots, \\ & \underline{\mu}_{\tilde{X}^p}(x_p), \overline{\mu}_{\tilde{F}_1^1}(x_1), \ldots, \overline{\mu}_{\tilde{F}_p^1}(x_p), \ldots, \overline{\mu}_{\tilde{F}_1^L}(x_1), \\ & \ldots, \overline{\mu}_{\tilde{F}_p^L}(x_p), \underline{\mu}_{\tilde{F}_1^{L+1}}(x_1), \ldots, \underline{\mu}_{\tilde{F}_p^{L+1}}(x_p), \ldots, \\ & \underline{\mu}_{\tilde{F}_1^M}(x_1), \ldots, \underline{\mu}_{\tilde{F}_p^M}(x_p), y_l^1, \ldots, y_l^M\Big). \end{aligned} \tag{57}$$

Similarly

$$\begin{aligned} y_r =& y_r\Big(\overline{\mu}_{\tilde{X}^1}(x_1), \ldots, \overline{\mu}_{\tilde{X}^p}(x_p), \underline{\mu}_{\tilde{X}^1}(x_1), \ldots, \\ & \underline{\mu}_{\tilde{X}^p}(x_p), \underline{\mu}_{\tilde{F}_1^1}(x_1), \ldots, \underline{\mu}_{\tilde{F}_p^1}(x_p), \ldots, \underline{\mu}_{\tilde{F}_1^R}(x_1), \\ & \ldots, \underline{\mu}_{\tilde{F}_p^R}(x_p), \overline{\mu}_{\tilde{F}_1^{R+1}}(x_1), \ldots, \overline{\mu}_{\tilde{F}_p^{R+1}}(x_p), \ldots, \\ & \overline{\mu}_{\tilde{F}_1^M}(x_1), \ldots, \overline{\mu}_{\tilde{F}_p^M}(x_p), y_r^1, \ldots, y_r^M\Big). \end{aligned} \tag{58}$$

8) Test each component of $\mathbf{x}$ to determine the active branches in $\underline{\mu}_{\tilde{F}_k^l}(x_k)$, $\underline{\mu}_{\tilde{X}_k}(x_k)$, $\overline{\mu}_{\tilde{F}_k^l}(x_k)$ and $\overline{\mu}_{\tilde{X}_k}(x_k)$, $k = 1, 2, \ldots, p$, and represent the active branches as functions of their associated parameters, e.g., use Tables I–III for the membership functions described in Example 4. This step depends on the locations of $\mathbf{x}$ in relation to the MFs.
9) Tune the parameters of the active branches and the parameters in the consequent using a steepest-descent (or any other optimization) method. The error function is (54).
10) Set $t \triangleq t+1$. If $t = T$, go to Step 11); otherwise go to Step 4).
11) Set $e \triangleq e+1$. If $e = E$, stop; otherwise, go to Step 3).

When the input is fuzzified to a type-1 fuzzy set, (57) and (58) are simplified since $\overline{\mu}_{\tilde{X}_k}(x_k) = \underline{\mu}_{\tilde{X}_k}(x_k)$, $k = 1, 2, \ldots, p$ or, if a singleton fuzzifier is used, (57) and (58) are simplified even further since all $\overline{\mu}_{\tilde{X}_k}(x_k)$ and $\underline{\mu}_{\tilde{X}_k}(x_k)$ disappear in (57) and (58), because $\overline{\mu}_{\tilde{X}_k}(x_k)$ and $\underline{\mu}_{\tilde{X}_k}(x_k)$ are two singletons.

What makes the tuning of the parameters of this type-2 FLS challenging and different from the tuning of the parameters in a type-1 FLS is having to first determine which parameters y_l and y_r depend on. This requires comparing x_k ($k = 1, 2, \ldots, p$) to some points associated with parameters of the upper and lower antecedent membership functions (e.g., as in Example 4). As these parameters change due to their tuning, it is highly likely that the dependency of y_l and y_r on parameters also changes. This behavior does not occur in a type-1 FLS.

VIII. Forecasting of Chaotic Time Series

Type-1 FLSs have been extensively used in time-series forecasting (e.g., [7], [8], [22], [24]). Here, we evaluate the performance of our design method by applying it to the forecasting of a Mackey–Glass chaotic time-series. We compare the performance of interval type-2 designs with that of type-1 designs.

A. Mackey–Glass Chaotic Time Series

The Mackey–Glass chaotic time series can be represented as [20]

$$\frac{ds(t)}{dt} = \frac{0.2s(t-\tau)}{1+s^{10}(t-\tau)} - 0.1s(t). \tag{59}$$

When $\tau > 17$, (59) exhibits chaotic behavior. In simulating (59), we converted it to a discrete-time equation by using Euler's method [30]. Denoting

$$f(s, n) = \frac{0.2s(n-\tau)}{1+s^{10}(n-\tau)} - 0.1s(n) \tag{60}$$

then

$$s(n+1) = s(n) + hf(s, n) \tag{61}$$

where h is a small number and the initial values of $s(n)$ $n \le \tau$ are set randomly. We chose $h = 1$ and $\tau = 30$.

In our simulations, we assumed that the sampled time-series $s(k)$ is corrupted by uniformly distributed additive noise $n(k)$ and only noisy measured values of $x(k)$ are available, i.e., $x(k) = s(k) + n(k)$, $k = 1, 2, \ldots, N$. In actual time-series such as the price curve for the U.S. dollar versus the German mark, market volatility can change noticeably over the course of time, so that the variance of the noise component, which is related to volatility, need not be constant [21]. In our simulation, we therefore assumed the noise is zero mean but has a signal-to-noise ratio (SNR) ranging from 0 dB [with standard deviation (std) $\sigma_{n_{0\,\mathrm{dB}}}$)] to 10 dB (with std $\sigma_{n_{10\,\mathrm{dB}}}$); it is uniformly distributed into 100 levels from $\sigma_{n_{0\,\mathrm{dB}}}$ to $\sigma_{n_{10\,\mathrm{dB}}}$ and

$$\sigma_n \triangleq \frac{\sigma_{n_{10\,\mathrm{dB}}} + \sigma_{n_{0\,\mathrm{dB}}}}{2}. \tag{62}$$

Our simulations were based on $N = 1000$ points, $x(1001)$, $x(1002)$, ..., $x(2000)$. The first 500 data $x(1001)$, $x(1002)$, ..., $x(1500)$ are for training and the remaining 500 data $x(1501)$, $x(1502)$, ..., $x(2000)$ are for testing. In Fig. 3(a), we plot the Mackey–Glass chaotic time series $s(1001)$, $s(1002)$, ..., $s(2000)$ and, in Fig. 3(b), we plot one realization of the noise corrupted data $x(1001)$, $x(1002)$, ..., $x(2000)$.

B. Simulations

We used four antecedents for forecasting, i.e., $x(k-3)$, $x(k-2)$, $x(k-1)$, and $x(k)$ were used to predict $x(k+1)$. As in [7], we used only two fuzzy sets for each antecedent, so the number of rules is $2^4 = 16$. The initial locations of antecedent MFs were based on the mean m_t and std σ_t of the first 500 points $x(1001)$, $x(1002)$, ..., $x(1500)$.

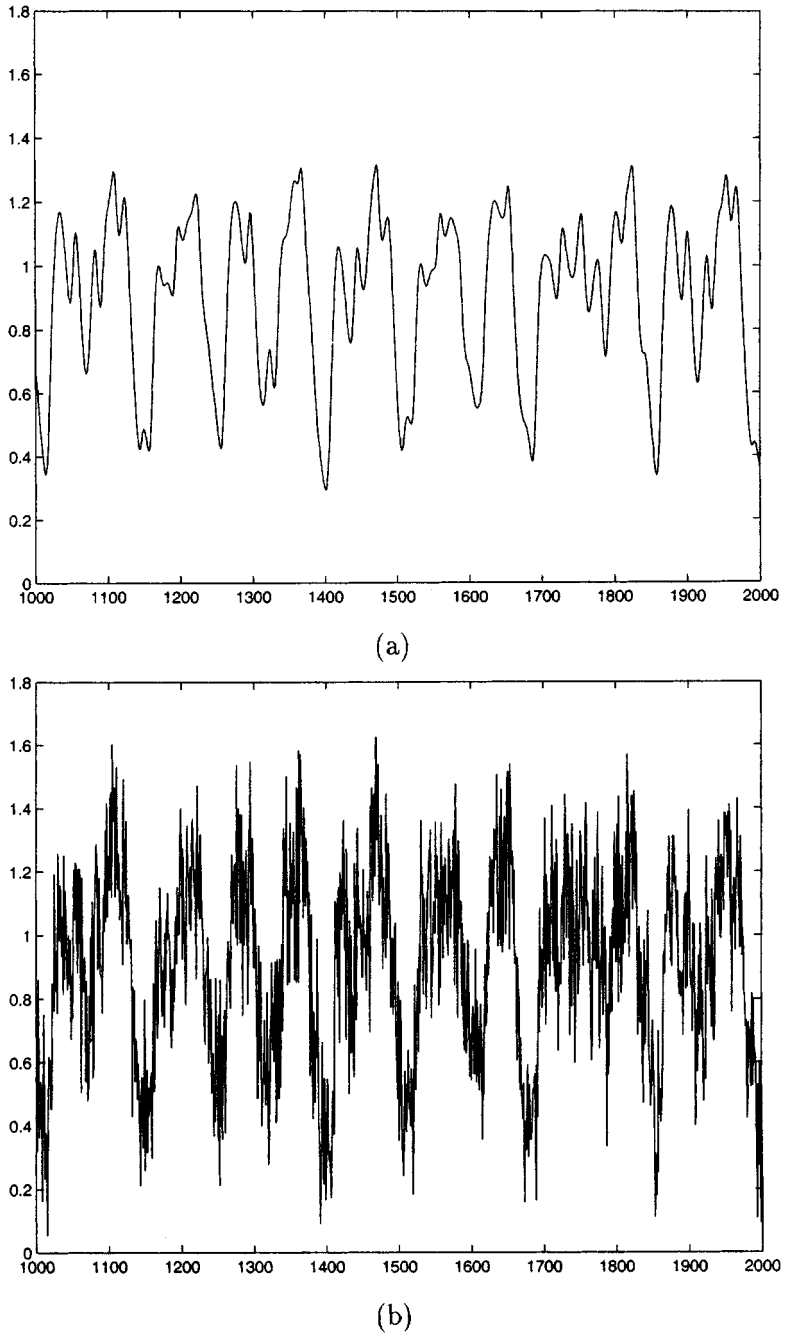

Fig. 3. The Mackey–Glass chaotic time series shows (a) the noise-free data $s(1001), s(1002), \ldots, s(2000)$ and (b) the noise corrupted data (in one realization), $x(1001), x(1002), \ldots, x(2000)$.

We compared the performance of the following five forecasting FLSs: type-1 singleton FLS (SFLS); type-1 non-singleton FLS (NSFLS),; type-2 SFLS; type-2 NSFLS with type-1 fuzzifier (type-2 NSFLS-1); and type-2 NSFLS with type-2 fuzzifier (type-2 NSFLS-2). Gaussian MFs were chosen for the antecedents of the type-1 FLSs; the Gaussian MFs of Example 1 were chosen for the *antecedents* of the type-2 FLSs; type-1 Gaussian MFs were chosen for the inputs of the type-1 NSFLS and type-2 NSFLS with type-1 fuzzifier and the Gaussian MFs of Example 2 were chosen for the *inputs* of the type-2 NSFLS with type-2 fuzzifier. The parameters and number of parameters in these five FLSs are summarized in Table IV [e.g., for the type-2 SFLS, total # of P= $(3 \times 4 + 2)16 = 224$]. The initial values of all the design parameters are summarized in Table V.

After training, the rules were fixed and we tested the fuzzy logic (FL) forecaster based on the remaining 500 noisy points, $x(1501), x(1502), \ldots, x(2000)$.

For each of the five designs, we ran 50 Monte-Carlo realizations and, for each realization, each FLS was tuned using a simple steepest-descent algorithm for six epochs. After each epoch, we used the testing data to see how each FLS performed

TABLE IV
THE PARAMETERS AND NUMBER OF PARAMETERS IN FIVE DIFFERENT FLSS (WITH 16 RULES AND FOUR ANTECEDENTS IN EACH RULE, I.E., $i = 1, \ldots, 16$, AND $k = 1, \ldots, 4$). P IS SHORT FOR *PARAMETERS*

FLS	P in one input set	P in one antecedent	P in one consequent	Total # of P
Type-1 SFLS	N/A	$m_{\mathrm{F}_k^i}$, $\sigma_{\mathrm{F}_k^i}$	$\overline{y}^i$	144
Type-1 NSFLS	σ_{X_k}	$m_{\mathrm{F}_k^i}$, $\sigma_{\mathrm{F}_k^i}$	$\overline{y}^i$	148
Type-2 SFLS	N/A	$m_{\tilde{\mathrm{F}}_{k1}^i}$, $m_{\tilde{\mathrm{F}}_{k2}^i}$, $\sigma_{\tilde{\mathrm{F}}_k^i}$	y_l^i, y_r^i	224
Type-2 NSFLS-1	σ_{X_k}	$m_{\tilde{\mathrm{F}}_{k1}^i}$, $m_{\tilde{\mathrm{F}}_{k2}^i}$, $\sigma_{\tilde{\mathrm{F}}_k^i}$	y_l^i, y_r^i	228
Type-2 NSFLS-2	$\sigma_{\tilde{\mathrm{X}}_{k1}}$, $\sigma_{\tilde{\mathrm{X}}_{k2}}$	$m_{\tilde{\mathrm{F}}_{k1}^i}$, $m_{\tilde{\mathrm{F}}_{k2}^i}$, $\sigma_{\tilde{\mathrm{F}}_k^i}$	y_l^i, y_r^i	232

TABLE V
INITIAL VALUES OF THE PARAMETERS IN FIVE FLSS. $m_{X_k} = m_{\tilde{X}_k} = x_k$ FOR ALL NSFLS DESIGNS. EACH ANTECEDENT IS DESCRIBED BY TWO FUZZY SETS

FLS	input	for each antecedent	consequent
Type-1 SFLS	N/A	mean: $m_t - 2\sigma_t$ or $m_t + 2\sigma_t$, $\sigma_{\mathrm{F}_k^i} = 2\sigma_t$	$\overline{y}^i \in [0, 1]$
Type-1 NSFLS	$\sigma_{\mathrm{X}_k} = \sigma_n$	mean: $m_t - 2\sigma_t$ or $m_t + 2\sigma_t$, $\sigma_{\mathrm{F}_k^i} = 2\sigma_t$	$\overline{y}^i \in [0, 1]$
Type-2 SFLS	N/A	mean: $[m_t - 2\sigma_t - 0.25\sigma_n, m_t - 2\sigma_t + 0.25\sigma_n]$ or $[m_t + 2\sigma_t - 0.25\sigma_n, m_t + 2\sigma_t + 0.25\sigma_n]$, $\sigma_{\tilde{\mathrm{F}}_k^i} = 2\sigma_t$	$y_l^i = \overline{y}^i - \sigma_n$, $y_r^i = \overline{y}^i + \sigma_n$
Type-2 NSFLS-1	$\sigma_{\mathrm{X}_k} = \sigma_n$	mean: $[m_t - 2\sigma_t - 0.25\sigma_n, m_t - 2\sigma_t + 0.25\sigma_n]$ or $[m_t + 2\sigma_t - 0.25\sigma_n, m_t + 2\sigma_t + 0.25\sigma_n]$, $\sigma_{\tilde{\mathrm{F}}_k^i} = 2\sigma_t$	$y_l^i = \overline{y}^i - \sigma_n$, $y_r^i = \overline{y}^i + \sigma_n$
Type-2 NSFLS-2	$\sigma_{\tilde{\mathrm{X}}_{k1}} = \sigma_{n_{10dB}}$, $\sigma_{\tilde{\mathrm{X}}_{k2}} = \sigma_{n_{0dB}}$	mean: $[m_t - 2\sigma_t - 0.25\sigma_n, m_t - 2\sigma_t + 0.25\sigma_n]$ or $[m_t + 2\sigma_t - 0.25\sigma_n, m_t + 2\sigma_t + 0.25\sigma_n]$, $\sigma_{\tilde{\mathrm{F}}_k^i} = 2\sigma_t$	$y_l^i = \overline{y}^i - \sigma_n$, $y_r^i = \overline{y}^i + \sigma_n$

by evaluating the rmse between the defuzzified output of each FLS and the noise-free data, i.e.,

$$\text{rmse} = \sqrt{\frac{1}{496} \sum_{k=1504}^{1999} [s(k+1) - f(\mathbf{x}^k)]^2} \qquad (63)$$

where $\mathbf{x}^k = [x(k-3), x(k-2), x(k-1), x(k)]^T$, and T denotes transpose.

Since there are $50 \times 6 = 300$ rmse values for each design, we summarize the mean and std of the rmses for each epoch and for each design in Fig. 4(a) and (b). Observe the following from the figures.

1) Type-2 FLSs outperform type-1 FLSs. The type-2 NSFLS-2 performs the best and the type-2 NSFLS-1 also gives very good results. The reason for the latter is because the type-2 NSFLS-1 uses σ_n in (62) as the initial std of the input sets and this value for σ_n gives a good approximation to the average value of the std of the uniform noise.
2) The type-2 FLSs (especially type-2 NSFLS-2) achieve close to their optimal performance almost at the first epoch of tuning. This property shows that type-2 FLSs (as compared to type-1 FLSs) are very promising for real-time signal processing where more than one epoch of tuning is not possible.
3) From the std of the rmses, we see that the type-2 FLSs (especially the type-2 NSFLS-2) have a considerably smaller std than do type-1 FLSs, which demonstrates that type-2 FLSs are much more robust to the noise than are type-1 FLSs. Hence, type-2 FLSs appear to be promising for use in adaptive filters such as channel equalizers (e.g., [29], [31], [38]) because such equalizers must be robust to additive noise.

IX. CONCLUSIONS AND FUTURE WORK

We have presented the theory and design of interval type-2 FLSs, including an efficient and simplified method to compute their input and antecedent operations. We have also provided a method for tuning the parameters of an interval type-2 FLS. Our simulation results show that an interval type-2 FLS outperforms a type-1 FLS in forecasting a chaotic time-series whose measurements were corrupted by *nonstationary* noise.

Interval type-2 FLSs provide a way to handle knowledge uncertainty. Data mining and knowledge discovery are important research topics that are being studied by researchers of neural networks, fuzzy logic systems, evolutionary computing, soft computing, artificial intelligence, etc. We believe that interval type-2 FLSs have the potential to solve data mining and knowledge discovery problems in the presence of uncertainty.

As we discussed, the large number of parameters and associated training complexity are the main disadvantages of interval type-2 FLSs. The challenge is to develop ways to reduce the number of parameters and training complexity. Some ways for reducing the number of design parameters that remain to be explored are: 1) assume the subsets in each antecedent are the same for all rules and 2) fix some parameters such as those in the membership functions of measured inputs.

We believe that promising areas in which type-2 FLSs may be advantageous over type-1 FLSs include mobile communications, communication networks, pattern recognition, and robust control because lots of uncertain information needs to be

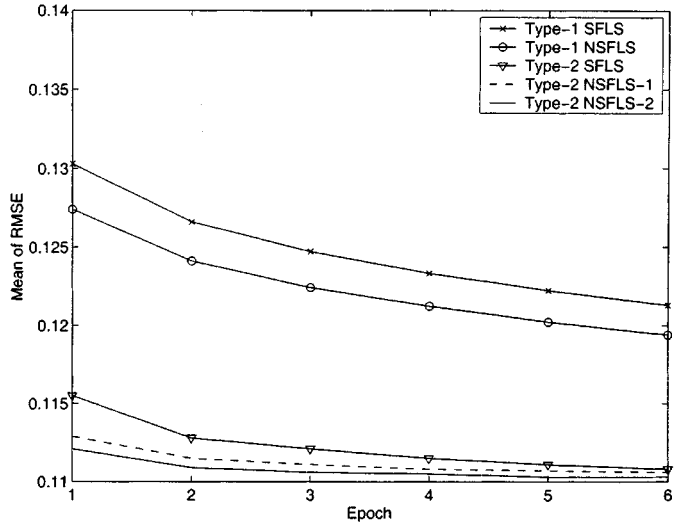

(a)

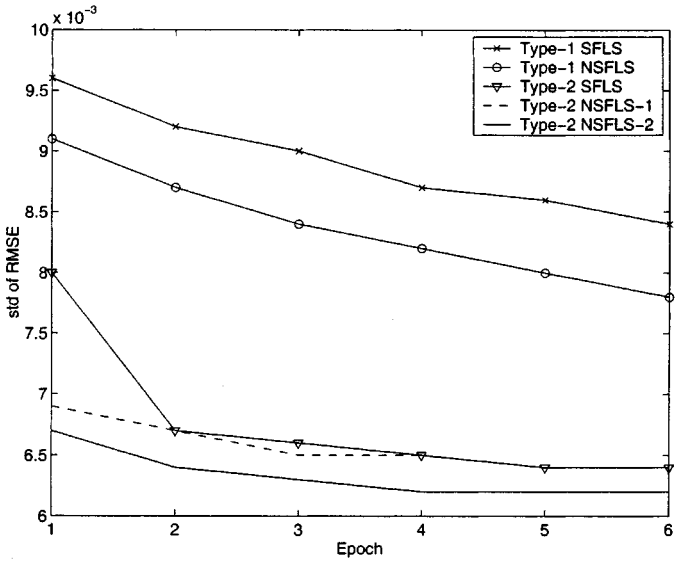

(b)

Fig. 4. The mean and std of the rmses (for the test data) for the five FLS designs averaged over 50 Monte-Carlo realizations. Tuning was performed in each realization for six epochs. (a) Mean values. (b) STD values.

handled in these areas. For example, in mobile communications, the fading channel coefficients are uncertain during adjacent training periods. Existing algorithms treat them as certain. In communication networks, Tanaka and Hosaka [5], [33] observed the difficulties of obtaining appropriate MFs for efficient network control, which suggests that type-2 MFs will be a better way to represent the uncertainty in such a network.

Finally, whether or not design procedures can be developed for noninterval type-2 FLSs remains to be explored.

APPENDIX A
DETAILS OF EXAMPLE 4

In determining $\overline{x}^l_{k,\max}$ and $\underline{x}^l_{k,\max}$, we need the calculation of the supremum of a product or minimum of two type-1 Gaussian MFs. Such a calculation has been carried out by Mouzouris and Mendel in [27] for the type-1 nonsingleton case; they derive the value of x_k at which $\sup_{x_k \in X_k} \int_{X_k} [\mu_{X_k}(x_k) \star \mu_{F^l_k}(x_k)]/x_k$ is achieved, where $\mu_{X_k}(x_k)$ and $\mu_{F^l_k}(x_k)$ are Gaussians. Denoting this value of x_k as $x^l_{k,\max}$, they have shown that for product t-norm

$$x^l_{k,\max} = \frac{\sigma^2_{X_k} m_{F^l_k} + \sigma^2_{F^l_k} m_{X_k}}{\sigma^2_{X_k} + \sigma^2_{F^l_k}} \tag{64}$$

and for minimum t-norm

$$x^l_{k,\max} = \frac{\sigma_{X_k} m_{F^l_k} + \sigma_{F^l_k} m_{X_k}}{\sigma_{X_k} + \sigma_{F^l_k}}. \tag{65}$$

A. Determination of $\overline{x}^l_{k,\max}$

To determine $\overline{x}^l_{k,\max}$, we need to consider three cases of different $m_{\tilde{X}_k}$ locations:

1) $m_{\tilde{X}_k} \le m_{\tilde{F}^i_{k1}}$: This case is depicted in Fig. 5(a) (the solid lines). As we see from (17), the active branch in the upper MF of the antecedent comes from

$$\exp\left[-\frac{1}{2}\left(\frac{x_k - m_{\tilde{F}^i_{k1}}}{\sigma_{\tilde{F}^i_k}}\right)^2\right]$$

so it is very straightforward to obtain $\overline{x}^l_{k,\max}$ based on (64) or (65). The result is given in Case 1 in Table I. It is easy to verify that $\overline{x}^l_{k,\max} \le m_{\tilde{F}^i_{k1}}$ for both product and minimum t-norm.

2) $m_{\tilde{X}_k} \in [m_{\tilde{F}^i_{k1}}, m_{\tilde{F}^i_{k2}}]$. This case is depicted in Fig. 5(b)–(d) (these three possible cases are needed to determine $\underline{x}^l_{k,\max}$, as we explain below, but the same result is obtained for $\overline{x}^l_{k,\max}$ in all three cases). As we see from Example 1, in all three cases, the active branch in the upper MF of the antecedent comes from the constant MF $\mu_{\tilde{F}^l_k}(x_k) = 1$ and, since $\overline{\mu}_{\tilde{X}_k}(m_{\tilde{X}_k}) = 1$, so $\overline{x}^l_{k,\max} = m_{\tilde{X}_k}$, which leads to $\mu_{\tilde{F}^l_k}(\overline{x}^l_{k,\max})$ $\overline{\mu}_{\tilde{X}_k}(\overline{x}^l_{k,\max}) = 1$. This result is given in Case 2 in Table I.

3) $m_{\tilde{X}_k} \ge m_{\tilde{F}^i_{k2}}$: This case is depicted in Fig. 5(e). The analysis for this case is very similar to that in Part I and the result is given in Case 3 in Table I.

B. Determination of $\underline{x}^l_{k,\max}$

1) Product t-Norm: To determine $\underline{x}^l_{k,\max}$ under product t-norm, we again need to consider three cases of $m_{\tilde{X}_k}$ locations.

As we see from (18), the lower MF of the antecedent comes from the intersection of two Gaussian MFs and that intersection point is $(m_{\tilde{F}^i_{k1}} + m_{\tilde{F}^i_{k2}})/2$. When $x_k \le (m_{\tilde{F}^i_{k1}} + m_{\tilde{F}^i_{k2}})/2$, the active branch is $\mathcal{N}(m_{\tilde{F}^i_{k2}}, \sigma_{\tilde{F}^i_k};\ x_k)$ and, when $x_k \ge (m_{\tilde{F}^i_{k1}} + m_{\tilde{F}^i_{k2}})/2$, the active branch is $\mathcal{N}(m_{\tilde{F}^i_{k1}}, \sigma_{\tilde{F}^i_k};\ x_k)$.

1) For the cases depicted in Fig. 5(a) and (b), $\underline{x}^l_{k,\max}$ involves the lower MF $\underline{\mu}_{\tilde{X}_k}$ and $\mathcal{N}(m_{\tilde{F}^i_{k2}}, \sigma_{\tilde{F}^i_k}; x_k)$, i.e., $\underline{x}^l_{k,\max} = (\sigma^2_{\tilde{X}_{k1}} m_{\tilde{F}^i_{k2}} + \sigma^2_{\tilde{F}^i_k} m_{\tilde{X}_k})/(\sigma^2_{\tilde{X}_{k1}} + \sigma^2_{\tilde{F}^i_k})$. For

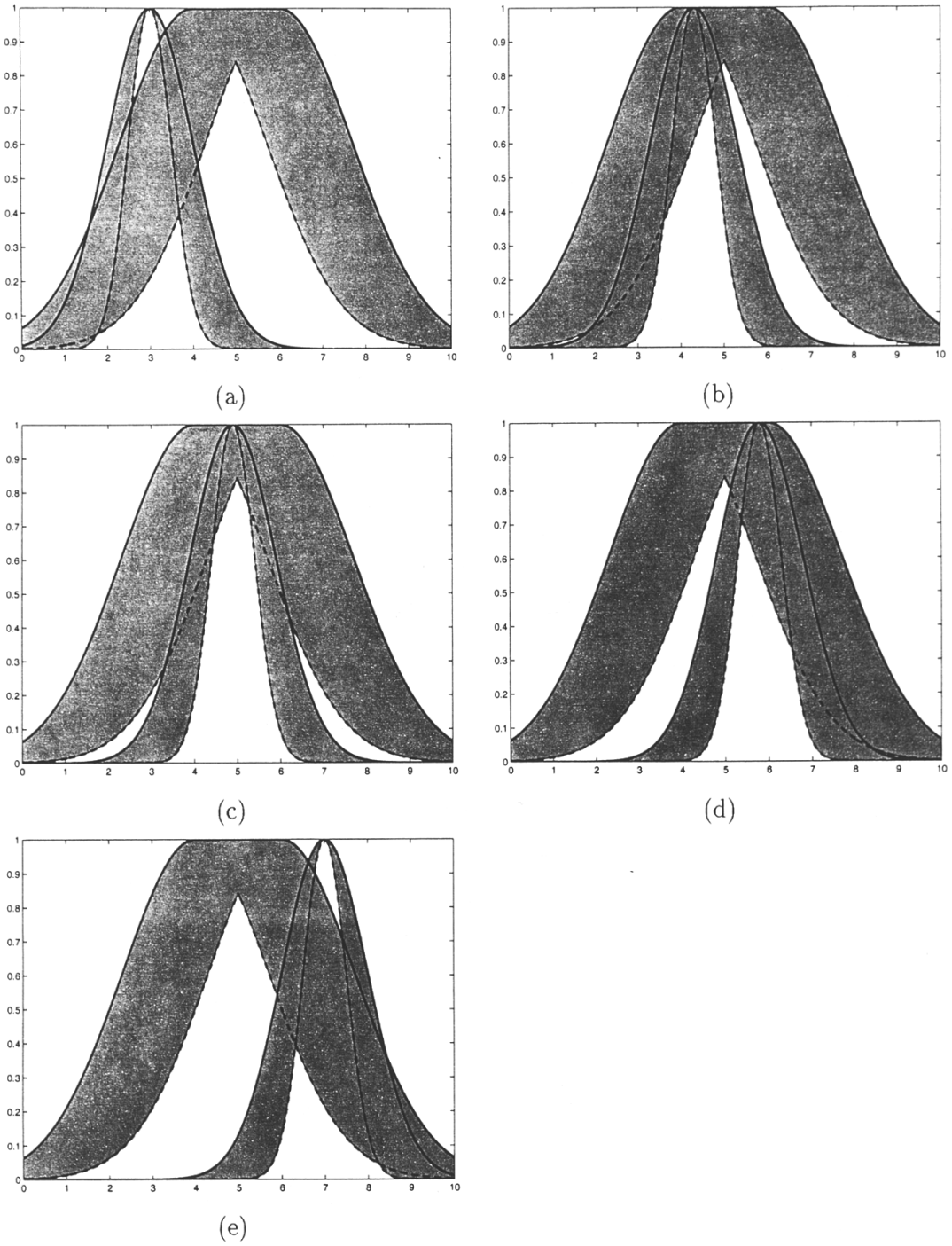

Fig. 5. In Example 4, possible locations of input type-2 MF and antecedent type-2 MF. The MF with the large footprint and variance is the antecedent MF, and the other is the input MF. (a)–(e) Cases 1-5, respectively.

this point to be located to the left of $(m_{\tilde{F}_{k1}^i} + m_{\tilde{F}_{k2}^i})/2$, we require

$$\frac{\sigma_{\tilde{X}_{k1}}^2 m_{\tilde{F}_{k2}^i} + \sigma_{\tilde{F}_k^i}^2 m_{\tilde{X}_k}}{\sigma_{\tilde{X}_{k1}}^2 + \sigma_{\tilde{F}_k^i}^2} \leq \frac{m_{\tilde{F}_{k1}^i} + m_{\tilde{F}_{k2}^i}}{2} \tag{66}$$

so that

$$m_{\tilde{X}_k} \leq \frac{m_{\tilde{F}_{k1}^i} + m_{\tilde{F}_{k2}^i}}{2} - \frac{\sigma_{\tilde{X}_{k1}}^2 \left(m_{\tilde{F}_{k2}^i} - m_{\tilde{F}_{k1}^i}\right)}{2\sigma_{\tilde{F}_k^i}^2}. \tag{67}$$

This result is given in Case 1 in Table II.

2) For the cases depicted in Fig. 5(d) and (e), $\underline{x}_{k,\max}^{l}$ involves the lower MF $\underline{\mu}_{\tilde{X}_k}$ and $\mathcal{N}(m_{\tilde{F}_{k1}^i}, \sigma_{\tilde{F}_k^i}; x_k)$. The analysis for this part is very similar to that for item 1 and we give the result in Table II, Case 3.
3) For the case depicted in Fig. 5(c) based on our results in Table II, Cases 1 and 3, $(m_{\tilde{F}_{k1}^i} + m_{\tilde{F}_{k2}^i})/2 - \sigma_{\tilde{X}_{k1}}^2 (m_{\tilde{F}_{k2}^i} - m_{\tilde{F}_{k1}^i})/2\sigma_{\tilde{F}_k^i}^2 \leq m_{\tilde{X}_k} \leq (m_{\tilde{F}_{k1}^i} + m_{\tilde{F}_{k2}^i})/2 + \sigma_{\tilde{X}_{k1}}^2 (m_{\tilde{F}_{k2}^i} - m_{\tilde{F}_{k1}^i})/2\sigma_{\tilde{F}_k^i}^2$. In this case, the

supremum point of the product between the lower MF $\underline{\mu}_{\tilde{X}_k}$ and $\mathcal{N}(m_{\tilde{F}^i_{k2}}, \sigma_{\tilde{F}^i_k}; x_k)$ is located to the right of or at $(m_{\tilde{F}^i_{k1}} + m_{\tilde{F}^i_{k2}})/2$ (recall Case 1), but $\mathcal{N}(m_{\tilde{F}^i_{k2}}, \sigma_{\tilde{F}^i_k}; x_k)$ is only active when $x_k \leq (m_{\tilde{F}^i_{k1}} + m_{\tilde{F}^i_{k2}})/2$. As we know, the product of two Gaussian MFs is convex and, to the left of the supremum point, it is monotonically increasing. Hence, the supremum point of the product between the lower MF $\underline{\mu}_{\tilde{X}_k}$ and $\mathcal{N}(m_{\tilde{F}^i_{k2}}, \sigma_{\tilde{F}^i_k}; x_k)$ $[x_k \leq (m_{\tilde{F}^i_{k1}} + m_{\tilde{F}^i_{k2}})/2]$ is at $(m_{\tilde{F}^i_{k1}} + m_{\tilde{F}^i_{k2}})/2$.

Additionally, the supremum point of the product between the lower MF $\underline{\mu}_{\tilde{X}_k}$ and $\mathcal{N}(m_{\tilde{F}^i_{k1}}, \sigma_{\tilde{F}^i_k}, x_k)$, is located to the left of or at $(m_{\tilde{F}^i_{k1}} + m_{\tilde{F}^i_{k2}})/2$ (recall Case 2). Hence, similar to the above analysis, the supremum point of the product between the lower MF $\underline{\mu}_{\tilde{X}_k}$ and $\mathcal{N}(m_{\tilde{F}^i_{k1}}, \sigma_{\tilde{F}^i_k} x_k)$ $[x_k \geq (m_{\tilde{F}^i_{k1}} + m_{\tilde{F}^i_{k2}})/2]$ is at $(m_{\tilde{F}^i_{k1}} + m_{\tilde{F}^i_{k2}})/2$.

Hence,

$$\underline{x}^l_{k,\max} = \frac{m_{\tilde{F}^i_{k1}} + m_{\tilde{F}^i_{k2}}}{2}. \tag{68}$$

This result is given in Table II, Case 2.

2) Minimum t-Norm: The results to obtain $\underline{x}^l_{k,\max}$ under minimum t-norm are given in Table III. The steps to obtain these results are exactly the same as those used to obtain the results in Table II and are left to the reader.

REFERENCES

[1] J. L. Chaneau, M. Gunaratne, and A. G. Altschaeffl, "An application of type-2 sets to decision making in engineering," in *Analysis of Fuzzy Information—Vol. II: Artificial Intelligence and Decision Systems*, J. C. Bezdek, Ed. Boca Raton, FL: CRC, 1987.

[2] D. Dubois and H. Prade, "Operations on fuzzy numbers," *Int. J. Syst. Sci.*, vol. 9, pp. 613–626, 1978.

[3] ——, "Operations in a fuzzy-valued logic," *Inform. Contr.*, vol. 43, pp. 224–240, 1979.

[4] ——, *Fuzzy Sets and Systems: Theory and Applications*. New York: Academic, 1980.

[5] S. Ghosh, Q. Razouqi, H. J. Schumacher, and A. Celmins, "A survey of recent advances in fuzzy logic in telecommunications networks and new challenges," *IEEE Trans. Fuzzy Syst.*, vol. 6, pp. 443–447, Aug. 1998.

[6] E. Hisdal, "The IF THEN ELSE statement and interval-valued fuzzy sets of higher type," *Int. J. Man–Machine Studies*, vol. 15, pp. 385–455, 1981.

[7] J.-S. R. Jang, "ANFIS: Adaptive-network-based fuzzy inference system," *IEEE Trans. Syst., Man, Cybern.*, vol. 23, pp. 665–685, May/June 1993.

[8] J.-S. R. Jang and C. -T. Sun, "Neuro-fuzzy modeling and control," *Proc. IEEE*, vol. 83, pp. 378–406, Mar. 1995.

[9] R. I. John, P. R. Innocent, and M. R. Barnes, "Type 2 fuzzy sets and neuro-fuzzy clustering of radiographic tibia images," in *Proc. 1998 IEEE Int. Conf. Fuzzy Syst.*, Anchorage, AK, May 1998, pp. 1373–1376.

[10] N. N. Karnik and J. M. Mendel, "Introduction to type-2 fuzzy logic systems," in *Proc. IEEE FUZZ Conf.*, Anchorage, AK, May 1998.

[11] ——, "Type-2 fuzzy logic systems: Type-reduction," in *IEEE Syst., Man, Cybern. Conf.*, San Diego, CA, Oct. 1998.

[12] ——, "An introduction to type-2 fuzzy logic systems,", USC Report, http://sipi.usc.edu/~mendel/report, Oct. 1998.

[13] ——, "Applications of type-2 fuzzy logic systems: handling the uncertainty associated with surveys," in *Proc. FUZZ-IEEE Conf.*, Seoul, Korea, Aug. 1999.

[14] ——, "Applications of type-2 fuzzy logic systems to forecasting of time-series," *Inform. Sci.*, vol. 120, pp. 89–111, 1999.

[15] ——, "Operations on type-2 fuzzy sets," Fuzzy Sets Syst., 2000, to be published.

[16] N. N. Karnik, J. M. Mendel, and Q. Liang, "Centroid of a type-2 fuzzy set," Inform. Sci., submitted for publication.

[17] ——, "Type-2 fuzzy logic systems," *IEEE Trans. Fuzzy Syst.*, vol. 7, pp. 643–658, Dec. 1999.

[18] A. Kaufmann and M. M. Gupta, *Introduction to Fuzzy Arithmetic: Theory and Applications*. New York: Van Nostrand Reinhold, 1991.

[19] C.-T. Lin and C. S. G. Lee, *Neural Fuzzy Systems*. Englewood Cliffs, NJ: Prentice-Hall, 1996.

[20] M. C. Mackey and L. Glass, "Oscillation and chaos in physiological control systems," *Sci.*, vol. 197, pp. 287–289, 1987.

[21] M. Magdon-Ismail, A. Nicholson, and Y. Abu-Mostafa, "Financial markets: Very noisy information processing," *Proc. IEEE*, vol. 86, pp. 2184–2195, Nov. 1998.

[22] J. M. Mendel, "Fuzzy logic systems for engineering: A tutorial," *Proc. IEEE*, vol. 83, pp. 345–377, Mar. 1995.

[23] ——, "Computing with words when words can mean different things to different people," in *Int. ICSC Congress Computat. Intell.: Methods Applicat., 3rd Annu. Symp. Fuzzy Logic Applicat.*, Rochester, NY, June 1999.

[24] J. M. Mendel and G. Mouzouris, "Designing fuzzy logic systems," *IEEE Trans. Circuits Syst. II*, vol. 44, pp. 885–895, Nov. 1997.

[25] M. Mizumoto and K. Tanaka, "Some properties of fuzzy sets of type 2," *Inform. Contr.*, vol. 31, pp. 312–340, 1976.

[26] ——, "Fuzzy sets of type 2 under algebraic product and algebraic sum," *Fuzzy Sets Syst.*, vol. 5, pp. 277–290, 1981.

[27] G. C. Mouzouris and J. M. Mendel, "Nonsingleton fuzzy logic systems: Theory and application," *IEEE Trans. Fuzzy Syst.*, vol. 5, pp. 56–71, Feb. 1997.

[28] J. Nieminen, "On the algebraic structure of fuzzy sets of type-2," *Kybernetica*, vol. 13, no. 4, Feb. 1977.

[29] S. K. Patra and B. Mulgrew, "Efficient architecture for Bayesian equalization using fuzzy filters," *IEEE Trans. Circuits Syst. II*, vol. 45, pp. 812–820, July 1998.

[30] D. Quinney, *An Introduction to the Numerical Solution of Differential Equation*. Hertforshire, U.K.: Research Studies, 1985.

[31] P. Sarwal and M. D. Srinath, "A fuzzy logic system for channel equalization," *IEEE Trans. Fuzzy Syst.*, vol. 3, pp. 246–249, May 1995.

[32] D. G. Schwartz, "The case for an interval-based representation of linguistic truth," *Fuzzy Sets Syst.*, vol. 17, pp. 153–165, 1985.

[33] Y. Tanaka and S. Hosaka, "Fuzzy control of telecommunications networks using learning technique," *Electron. Communicat. Japan*, pt. I, vol. 76, no. 12, pp. 41–51, Dec. 1993.

[34] I. Turksen, "Interval valued fuzzy sets based on normal forms," *Fuzzy Sets Syst.*, vol. 20, pp. 191–210, 1986.

[35] M. Wagenknecht and K. Hartmann, "Application of fuzzy sets of type 2 to the solution of fuzzy equation systems," *Fuzzy Sets Syst.*, vol. 25, pp. 183–190, 1988.

[36] L.-X. Wang and J. M. Mendel, "Back-propagation of fuzzy systems as nonlinear dynamic system identifiers," in *Proc. IEEE Int. Conf. Fuzzy Syst.*, San Diego, CA, Mar. 1992, pp. 1409–1418.

[37] ——, "Fuzzy basis functions, universal approximation, and orthogonal least squares learning," *IEEE Trans. Neural Networks*, vol. 3, pp. 807–814, Sept. 1992.

[38] ——, "Fuzzy adaptive filters, with application to nonlinear channel equalization," *IEEE Trans. Fuzzy Syst.*, vol. 1, pp. 161–170, Aug. 1993.

[39] K. C. Wu, "Fuzzy interval control of mobile robots," *Comput. Elect. Eng.*, vol. 22, no. 3, pp. 211–229, 1996.

[40] R. R. Yager, "Fuzzy subsets of type II in decisions," *J. Cybern.*, vol. 10, pp. 137–159, 1980.

[41] L. A. Zadeh, "The concept of a linguistic variable and its application to approximate reasoning—I," *Inform. Sci.*, vol. 8, pp. 199–249, 1975.

[42] H. J. Zimmermann, *Fuzzy Set Theory and Its Applications*, 2nd ed. Boston, MA: Kluwer, 1991.

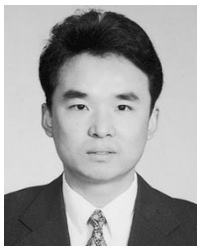

Qilian Liang received the B.S. degree from Wuhan University, China, in 1993, the M.S. degree from Beijing University of Posts and Telecommunications, China, in 1996, and the Ph.D. degree from University of Southern California, Los Angeles, in 2000, all in electrical engineering.

He was a Research Assistant in the Department of Electrical Engineering-Systems, University of Southern California, Los Angeles, from September 1997 to May 2000. His research interests include wireless communications, broad-band networks, fuzzy logic systems, and video traffic classification. He is currently with Hughes Network Systems, San Diego, CA.

Jerry M. Mendel (S'59–M'61–SM'72–F'78) received the Ph.D. degree in electrical engineering from the Polytechnic Institute of Brooklyn, Brooklyn, NY.

Currently, he is Professor of Electrical Engineering and Associate Director for Education of the Integrated Media Systems Center at the University of Southern California, Los Angeles, where he has been since 1974. He has published over 380 technical papers and is author and/or editor of seven books. His present research interests include type-2 fuzzy logic systems and their applications to a wide range of problems.

Dr. Mendel is a Distinguished Member of the IEEE Control Systems Society. He was President of the IEEE Control Systems Society in 1986. Among his awards are the 1983 Best Transactions Paper Award of the IEEE Geoscience and Remote Sensing Society, the 1992 Signal Processing Society Paper Award, a 1984 IEEE Centennial Medal, and an IEEE Third Millenium Medal.